Green Chemistry

PAPER

View Article Online
View Journal | View Issue

Cite this: *Green Chem.*, 2024, **26**, 7067

Characterization of polymer properties and identification of additives in commercially available research plastics†

Amy A. Cuthbertson,[a,b] Clarissa Lincoln,[a,b] Joel Miscall,[a,b] Lisa M. Stanley,[a] Anjani K. Maurya,[b,c] Arun S. Asundi,[b,c] Christopher J. Tassone,[b,c] Nicholas A. Rorrer *[a,b] and Gregg T. Beckham *[a,b]

For polymer recycling research, consistent polymer substrates sourced from widely available vendors are useful to enable direct comparisons between studies. Additionally, when reporting new recycling approaches, it is essential to characterize polymer chemical composition, physical properties, structure, and the presence of additives. Here we characterized 59 polymers from common commercial vendors across 20 different polymer classes, representing >95% of global plastic production by mass. Structural characterization was conducted with gel permeation chromatography, Fourier-transform infrared spectroscopy, and small and wide-angle X-ray scattering, and bulk characterization included CHNS measurements and elemental analysis by inductively coupled plasma mass spectrometry (ICP-MS). Thermal properties were measured using differential scanning calorimetry (DSC) and thermal gravimetric analysis. Nearly all plastics studied contained inorganic and organic additives, including halogens, sulfur-containing compounds, and antioxidants, which were investigated by either ICP-MS, accelerated solvent extraction followed by gas chromatography-mass spectrometry (GC-MS), pyrolysis GC-MS and high-resolution GC-MS. In general, the polymers vary from what they were reported to be, with 5 polymers exhibiting molar mass distributions different from that provided by vendors, 6 polymers exhibiting bimodal molecular mass distributions, and 10 polymers displaying unexpected thermal properties measured by DSC including multiple glass transitions and unusual exotherms. Finally, we also investigated changes in properties pre- and post-cryomilling, a common preprocessing technique in recycling studies. Here we found that 16 polymers had changes in either the average molecular mass, dispersity, or percent crystallinity after cryomilling. Taken together, this study further highlights the need to conduct thorough characterization on polymer substates while also providing a baseline analytical characterization for widely available research plastics. We have further made all data available through an online database.

Received 4th February 2024,
Accepted 21st March 2024

DOI: 10.1039/d4gc00659c

rsc.li/greenchem

Introduction

As a result of the global plastics waste challenge, new processes for plastics recycling are actively being pursued.[1–7] While mechanical recycling is primarily applicable to polyethylene terephthalate (PET) bottles, high-density polyethylene (HDPE), and polypropylene (PP) containers,[8–10] plastics exhibit a much broader chemical diversity than these three polymers and are also commonly formulated with multiple polymers, adhesives, and small molecule additives, generating complex waste streams.[1,11] Key to making rapid progress in the development of new recycling approaches are the needs for (1) rigorous substrate characterization, (2) an understanding of how polymer properties and additives influence recycling processes, and (3) the use of globally-available benchmark substrates that enable direct comparison between studies.[1] For instance, low concentrations of additives such as metals, sulfides, or antioxidants may interfere with new recycling processes.[1,12,13] As examples, Hinton *et al.* demonstrated that antioxidants (0.5–2 wt%) significantly impact the product yields in catalytic hydrocracking of HDPE,[14] and similarly, Jerdy *et al.* showed that antioxidants, and acid scavengers hindered the catalytic upgrading of HDPE plastic pyrolysis oil.[13]

[a]*Renewable Resources and Enabling Sciences Center, National Renewable Energy Laboratory, Golden, CO, 80401, USA. E-mail: nicholas.rorrer@nrel.gov, gregg.beckham@nrel.gov*
[b]*BOTTLE Consortium, Golden, CO 80401, USA*
[c]*Stanford Synchrotron Radiation Lightsource, SLAC National Accelerator Laboratory, Menlo Park, CA 94025, USA*

† Electronic supplementary information (ESI) available. See DOI: https://doi.org/10.1039/d4gc00659c

Furthermore, physical properties such as molecular mass, branch density and percent crystallinity can impact product yields during catalytic and enzymatic deconstruction of polymers.[15,16]

Approximately 95% of all plastics manufactured globally in 2018 by production capacity can be attributed to the 20 polymer types represented in Fig. 1.[1,17] However, these polymer classes do not fully indicate the complexity of plastics compositions or formulations. A recent review classified 10 547 unique chemicals associated with use in plastics, as either monomers, additives, or processing aids.[18] Of these, 25% were substances of unknown or variable composition, with most of the rest classified as individual compounds. Most plastic additives can be divided into 4 categories: (1) functional additives (*e.g.* stabilizers, antistatic agents, flame retardants, plasticizers, lubricants *etc.*), (2) colorants (*e.g.* pigments, dyes), (3) fillers (*e.g.* $CaCO_3$, talc, *etc.*), and (4) reinforcements (*e.g.* glass fiber, carbon fiber, *etc.*). The most commonly used additives are plasticizers, flame retardants, antioxidants, acid scavengers, UV and thermal stabilizers, lubricants, pigments, antistatic agents, and slip agents.[19,20] While there are many studies on plastic additives found in the natural environment,[21–24] there are considerably fewer studies on the occurrence of additives in manufactured plastics in relation to the development of new recycling strategies.[25–27]

In this study, we aimed to provide baseline data for polymers that are available commercially and commonly used as benchmark substrates for research. To that end, we comprehensively characterized 59 polymers across 20 polymer classes, sourced from widely available commercial vendors, including Alfa Aesar, Goodfellow, and Sigma-Aldrich, among others (Table 1). We characterized molecular composition, polymer morphology, molecular mass distributions, thermal properties, elemental compositions, the presence of additives, and the effects of cryomilling on structural and thermal properties. All source data are available in the ESI† or provided online. Taken together, we intend this work to provide both baseline analytical characterization of plastics and plastic additives for recycling studies and a resource on how to comprehensively perform these characterizations, as well as providing the research community with readily accessible fully characterized substrates.

Results

Similar to how studies in the biomass conversion literature report baseline characterization data, for polymer recycling research, it is critical to both use benchmark substrates from

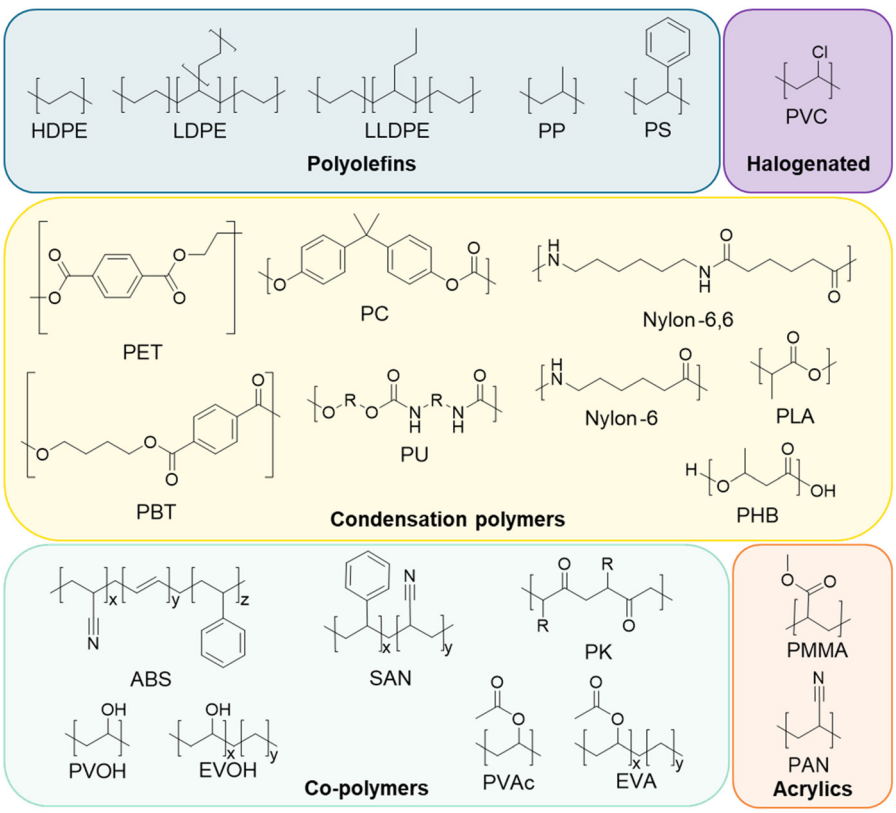

Fig. 1 Chemical classes of plastics analyzed in this study. Abbreviations: high-density polyethylene (HDPE), low-density polyethylene (LDPE), linear low-density polyethylene (LLDPE), polypropylene (PP), polystyrene (PS), polyvinyl chloride (PVC), polyethylene terephthalate (PET), polycarbonate (PC), nylon-6,6, polybutylene terephthalate (PBT), polyurethane (PU), nylon-6, polylactic acid (PLA), polyhydroxybutyrate (PHB), acrylonitrile butadiene styrene (ABS), styrene acrylonitrile (SAN), polyketone (PK), polyvinyl alcohol (PVOH), ethylene vinyl alcohol (EVOH), polyvinyl acetate (PVAc), ethylene vinyl acetate (EVA), polymethyl methacyrlate (PMMA), and polyacrylonitrile (PAN).

Table 1 Polymer data for 59 substrates including sample code, supplier product and lot numbers (when accessible), supplier description (including when available: particle size, weight-average molecular mass (M_w), number-average molecular mass (M_n), additive content, glass transition temperature (T_g) determined by DSC at 10 °C min^{-1}, crystallinity temperature (T_c), *etc.*), experimental M_w, dispersity ($Đ$), T_g, melting temperature (T_m) at peak maximum with %crystallinity, elemental composition by weight percent (wt%), and list of probable extractable additives. Measurements of polymers represented are for as received or non-cryomilled, unless otherwise annotated. For substrates with significant bimodal distributions, M_w and $Đ$ are given for both peaks

Polymer type	Sample code	Supplier, product number, lot number	Supplier description	M_w (kDa), $Đ$	T_g (°C)[a,b]	T_m (°C), % crystallinity[c]	CHNS, F, and ICP-MS elemental composition (wt%), total wt%	Probable extractable additives
Polyethylene	PE-1	Alfa Aesar, 41731, S02D047	High density granules, 125 kDa, white, 0.34% volatiles	90.9, 3.2	41	130.7, 57.2%	C (85.15), H (13.39), S (0.12), B (0.034),[d] Na (0.006), Al (0.006), Si (1.593), 100.299%	Wax mixture
	PE-2	NIST, SRM-1475	M_w 53 kDa pellet, Irganox 1010 at 111 ppm	23.5, 9.3	46[a]	136.3, 77.6%	C (83.67), H (13.65), S (0.09), B (0.027),[d] Na (0.013), Al (0.005), Si (0.913), Ca,[d] 98.368%	Stabilizers, antioxidants, wax mixture, fatty acids
	PE-3	Alfa Aesar, 45085, W22A017	Medium density powder, 1.8 kDa, white, 0.43% volatiles	15.1, 2.0	53	112.3, 34.5%	C (82.77), H (13.77), S (0.10), F (0.10), B (0.044),[d] Na (0.005), Si (0.314), Ca,[d] 97.103%	Wax mixture
	PE-4	Goodfellow, ET316031/4	Low density powder, max particle size 300 μm, white	86.3, 2.6	47	103.7, 23.7%	C (85.15), H (14.02), S (0.09), F (0.20), B (0.034),[d] Si (0.085), Ca,[d] 99.498%	Minimal additives; hydrocarbons
	PE-5	Goodfellow, ET311452	Low density, film (0.5 mm) natural color	79.1, 1.9	44	113.8, 32.9%	C (85.43), H (14.00), B,[d] Na,[d] Mg[d] Al,[d] P,[d] 99.430%	Wax mixture, antioxidant, plasticizer, unknowns
	PE-6	Goodfellow, ET323100/16	1 mm high density sheet	136.4, 3.8	43	130.6, 50.2%	C (85.34), H (13.98), F (0.10), B (0.052),[d] Si (0.037), Ca,[d] Zn (0.010), W (0.007), 99.526%	Wax mixture, antioxidant, plasticizer
	PE-7	EDA Plastics	High density pellets, post-consumer recycled plastic milk and water bottles	91.1, 3.1	—	136.0, 63.2%	C (85.54), H (14.20), S (0.11), B (0.035),[d] Al (0.009), Si (0.020), Ca,[d] 99.914%	Wax mixture, unknowns
	PE-8	Goodfellow, ET316320	Low density granule, nominal granule size 2 mm, natural color	85.2, 2.0	43	115.6, 29.4%	C (85.35), H (14.01), S (0.11), B (0.043),[d] Mg (0.022), Si (0.016), Ca,[d] 99.551%	Unknown hydrocarbons
	PE-9	Goodfellow, EET316310/2	Low density granule, nominal granule size 5 mm, natural color, extrusion, and injection molding grade, melt flow rate 2	80.5, 2.0	40	113.6, 32.9%	C (85.57), H (14.00), S (0.11), F (0.10), B (0.045),[d] Si (0.007), Ca,[d] 99.832%	Phthalates, slip agents
	PE-10	Goodfellow, ET326310/10	High density granules, nominal granule size 2–4 mm, injection molding grade, melt flow rate 7.6	71.6, 1.8	—	137.2, 58.4%	C (85.42), H (14.12), S (0.11), B (0.039),[d] Ca,[d] 99.689%	Wax mixture
	PE-11	Goodfellow, ET3263203	High density granule, nominal granule size 5 mm, natural color, melt flow rate 0.2 190 °C 2.16 kg, extrusion, and blow molding grade	106.0, 2.4	—	134.6, 56.7%	C (85.43), H (13.91), S (0.16), F (0.16), B (0.039),[d] Ca,[d] 99.699%	Wax mixture, wax mixture, antioxidant, plasticizer
Polyethylene terephthalate	PET-1	Goodfellow; ES306031	Powder, white	35.2, 1.9	73	236.1, 41.8%	C (61.97), H (4.42), F (0.10), B (0.035),[d] Ca,[d] Sb (0.063), W (0.005), 66.593%	Unknowns
	PET-2	Goodfellow, ES301450	Film (0.25 mm), biaxial	24.8, 2.6	53[a]	257.7, 28.2%	C (62.16), H (4.74), B (0.025),[d] Ca,[d] Sb (0.013), 66.938%	Phthalates
	PET-3	Goodfellow, ES301445	Film (0.25 mm), natural color (not on label), amorphous	28.0, 1.7	70	248.0, 2.0%	C (62.38), H (4.58), F (0.10), B (0.024),[d] Na (0.015), Si (0.016), Ca,[d] Sb (0.025), 67.140%	Phthalates, unknowns

Table 1 *(Contd.)*

Polymer type	Sample code	Supplier, product number, lot number	Supplier description	M_w (kDa), $Đ$	T_g (°C)[a,b]	T_m (°C), % crystallinity[c]	CHNS, F, and ICP-MS elemental composition (wt%), total wt%	Probable extractable additives
Polypropylene	PP-1	Sigma Aldrich, 428116 – 250 g, MKCH4322	Isotactic, avg. M_w 12 kDa, avg. M_n 5 kDa, pellets, natural color	41.0, 1.6	59[a]	159.5, 48.1%	C (82.41), H (12.73), B (0.031),[d] Al (0.006), Ca,[d] Cl (0.010), 95.187%	Complex mixtures of wax and fatty acids, UV stabilizer
	PP-2	Sigma Aldrich, 428175 – 1 kg, MKCH0909	Amorphous pellets, natural color	47.2, 2.2	−12, 51	154.5, 10.2%	C (85.62), H (13.65), B (0.036),[d] Ca,[d] 99.306%	Complex wax mixture
	PP-3	Sigma Aldrich, 427888 – 1 kg, MKCH9443	Isotactic, avg. M_w 250 kDa, avg. M_n 67, pellets	190.9, 1.8	43	169.7, 43.1%	C (84.93), H (13.47), B (0.036),[d] Na (0.005), Ca,[d] 98.441%	Stabilizer or UV-absorber, wax mixture
	PP-4	Goodfellow, PP301350	Film (0.05 mm), clear/transparent	229.6, 1.9	45	165.8, 40.5%	C (84.93), H (13.74), N (0.19), F (0.10), B (0.035), Na (0.007), Mg (0.005), Al (0.006), Ca,[d] 99.013%	Plasticizer, antioxidant, wax mixture, unknowns
	PP-5	Goodfellow, PP306320/4	Granule, nominal granule size 3 mm, natural color, block co-polymer	337.0, 2.1	40	169.2, 37.1%	C (85.05), H (12.85), F (0.10), B (0.024), Na (0.008), Mg (0.081), Al (0.010), Si (0.009), Ca,[d] 98.132%	Fatty acids, low molecular weight polypropylene
	PP-6	Goodfellow, PP306315/1	Isotactic granule, nominal granule size 4 mm, natural color, T_g −26 °C	232.5, 2.0	73	167.0, 40.8%	C (85.63), H (13.35), F (0.10), B (0.028),[d] Ca,[d] 99.108%	Paraffin wax mixture, phthalates, unknowns
	PP-7	Goodfellow, PP306312/3	Granule, nominal granule size 5 mm, natural color, homopolymer, melt flow rate 6	214.5, 1.9	42	167.5, 41.2%	C (85.70), H (13.58), B (0.036),[d] Na (0.005), Al (0.034), Ca,[d] 99.355%	Unknown wax mixture, phosphite based stabilizer
Polyvinyl chloride	PVC-1	Goodfellow, CV316010/4	PVC unplasticized (UPVC), 250 μm powder, white, Norvinyl™ grade, <0.2% volatiles	(669.3, 2.9) (53.8, 2.4)	84	—	C (38.21), H (4.97), F (0.13), B (0.021),[d] Si (0.202), Ti (0.006), 43.539%	Plasticizers
	PVC-2	Goodfellow, CV313005/8	PVC unplasticized (UPVC), film (0.5 mm), white	74.8, 3.8	73	—	C (38.56), H (5.00), F (0.10), B (0.018),[d] Na (0.013), Al (0.076), Si (0.442), P (0.028), Ti (3.865), Sn (0.380), Sb (0.008), 48.490%	Maleic anhydride, antioxidants, plasticizers,
Polystyrene	PS-1	Sigma Aldrich, 82427 – 1 kg, MKCQ5090	280 kDa avg. M_w by GPC, pellets	258.9, 2.2	104	—	C (91.66), H (8.03), F (0.19), B (0.028),[d] Ca,[d] Zn (0.009), 99.917%	Unknowns
	PS-2	Goodfellow, ST316003/4	Amorphous powder, max particle size 900 μm, contains pentane, expandable pellet condition	209.6, 2.0	81, 113	—	C (91.57), H (8.26), F (0.19), B (0.034),[d] Ca,[d] Zn (0.011), 100.065%	Plasticizer, unknowns
	PS-3	Goodfellow	Biaxial	270.3, 2.8	105	—	C (90.97), H (7.92), F (0.10), B (0.037),[d] Ca,[d] Zn (0.009), 99.036%	Phthalates, unknowns
	PS-4	Goodfellow, ST316311/1	3–5 mm granules, melt flow rate 3.3, natural color	262.8, 2.0	105	—	C (91.84), H (8.07), F (0.10), B (0.030),[d] Zn (0.006), 100.046%	Unknowns
	PS-5	Sigma Aldrich, 331651 – 500 g, MKCG5477	35 kDa avg. M_w, pellet, or pellets, colorless	(113.6, 1.9) (1.8, 1.4)	61[b]	74.7[c]	C (91.61), H (8.06), B (0.028),[d] 99.698%	Mixture of aromatics, unknowns
Polyurethane	PU-1	Goodfellow, UR306300/2	Granule, nominal granule size 3–5 mm, natural color, thermoplastic elastomer, Ellastollan® L 1185 A12	556.7, 1.8	89	—	C (65.77), H (10.06), N (4.36), B (0.029),[d] Si (0.187), 80.406%	Antioxidants, plasticizers, surface sealer

Table 1 *(Contd.)*

Polymer type	Sample code	Supplier, product number, lot number	Supplier description	M_w (kDa), $Đ$	T_g (°C)[a,b]	T_m (°C), % crystallinity[c]	CHNS, F, and ICP-MS elemental composition (wt%), total wt%	Probable extractable additives
Acrylonitrile butadiene styrene	ABS-1		Black tubing	164.0, 4.2	69, 101	—	C (85.18), H (8.01), N (5.18), S (0.37), F (0.10), B (0.034),[d] Mg (0.012), Al (0.008), Si (0.411), Ti (0.007), Cr (0.012), Cl (0.156), 99.480%	Monomer and trimers, UV-absorbers, plasticizers, unknowns
	ABS-2	USA Ceiling	1/8 in. sheet, black	118.6, 5.8	72, 106	—	C (84.58), H (7.78), N (5.68), S (0.03), F (0.21), B (0.039),[d] Mg (0.034), Si (0.377), Ti (0.011), 98.741%	Monomer and trimers, plasticizers, unknowns
	ABS-3	USA Ceiling	1/8 in. sheet, yellow	224.6, 10.8	71, 108	—	C (84.96), H (8.43), N (5.31), S (0.07), F (0.11), B (0.014),[d] Mg (0.008), Si (0.203), P (0.005), Ti (0.012), Cl (0.011), 99.133%	Monomer and trimers, plasticizers, unknowns
Nylon	Nylon-6	Goodfellow, AM301400/7	PA6 0.5 mm film, translucent	38.1, 1.8	40, 66	215.2, 19.6%	C (63.22), H (9.72), N (12.11), B (0.035),[d] Si (0.130), Ti (0.005), 85.220%	Monomer, industrial side product, unknown
	Nylon-66	Goodfellow, AM321400	PA66 0.5 mm film, translucent	40.2, 1.6	61	257.8, 27.0%	C (62.44), H (9.06), N (11.96), S (0.75), F (0.10), B (0.030),[d] Na (0.005), Si (0.136), Ti (0.005), 84.486%	Industrial side product, plasticizer, unknowns
Polymethyl methacrylate	PMMA-1	Goodfellow, ME303906	Sheet (0.5 mm), clear/transparent, Hesaglas®VOS Grade (cast, not cross-linked)	2428.0, 2.3	109	—	C (61.05), H (8.15), F (0.10), B (0.032),[d] Si (0.232), Ti (0.009), 69.573%	Monomer, UV-absorber
	PMMA-2	Scientific Polymer Products Inc.	Powder	34.3, 1.5	79, 114	—	C (59.59), H (7.81), S (0.12), F (0.13), B (0.023),[d] Si (0.187), Ti (0.007), 67.867%	Monomer, slip agents, phthalates, unknowns
	PMMA-3	ePlastics	0.25 in. plate, clear	127.0, 1.8	67, 112	—	C (59.79), H (7.86), B (0.027),[d] Na (0.021), Al (0.009), Si (0.069), Ca,[d] 67.776%	Monomer, slip agents, UV-absorber, phthalates
	PMMA-4	ePlastics	Plate, 2283 red	1576.0, 2.8	64, 103	—	C (61.11), H (7.96), B (0.038),[d] Ca,[d] Ti (0.005), 69.113%	Monomer, red dye, slip agents, UV-absorber, phthalates
	PMMA-5	ePlastics	Plate, 2051 blue	1422.0, 2.6	66, 99	—	C (61.18), H (7.89), F (0.18), B (0.041),[d] 69.291%	Monomer, blue dye, slip agents, UV-absorber, phthalates
	PMMA-6	ePlastics	Plate, 2092 green	1767.0, 2.6	69, 115	—	C (59.90), H (7.93), B (0.039),[d] Ca,[d] Ti (0.006), 67.875%	Monomer, green dye, slip agents, UV-absorber, phthalates
Polycarbonate	PC-1	Goodfellow, CT301310	Film (0.175 mm), white (not on label)	8.1, 1.7	146	—	C (78.11), H (8.34), F (0.20), B (0.038),[d] Si (0.302), Ti (0.010), Cr (0.005), Cl (0.017), 87.022%	UV-absorber, phthalates, unknowns
Polyvinyl acetate	PVAc-1	Sigma Aldrich, 189480 – 500 g, MKCP8596	100 kDa by GPC pellets, colorless	101.9, 1.9	43	46.4[e], 5.5	C (55.65), H (6.84), F (0.10), B (0.021),[d] 62.611%	Plasticizer, aromatic unknowns,

Table 1 *(Contd.)*

Polymer type	Sample code	Supplier, product number, lot number	Supplier description	M_w (kDa), $Đ$	T_g (°C)[a,b]	T_m (°C), % crystallinity[c]	CHNS, F, and ICP-MS elemental composition (wt%), total wt%	Probable extractable additives
Ethylene vinyl acetate	EVA-1	Sigma Aldrich, 437220, MKCJ5370	25 wt% vinyl acetate pellets, colorless, melt index: 19 g/10 min @ 190 °C 2.16 kg, contains 200–900 ppm BHT as inhibitor	153.9, 2.5	−34	61.6	C (78.12), H (12.48), F (0.10), B (0.034),[d] Ca,[d] 90.734%	Butylated hydroxytoluene (antioxidant), phthalates
	EVA-2	Sigma Aldrich, 340502 – 250 g, MKCM5048	40% vinyl acetate pellets, colorless, melt index: 53 g/10 min @ 190 °C 2.16 kg, contains 200–800 ppm BHT as inhibitor, 0.2–0.6% "W" additive	113.2, 2.2	−33	47.8	C (73.40), H (11.37), F (0.12), B (0.028),[d] Ca,[d] 84.918%	Butylated hydroxytoluene (antioxidant), wax mixture
	EVA-3	Goodfellow, ET346300/1	3–5 mm granules, yellow universal masterbatch	(171.2, 1.5) (0.5, 1.3)	41	75.4	C (70.44), H (7.10), N (0.88), S (0.41), F (0.10), B (0.017),[d] Na (0.017), Al (0.046), P (0.023), Ca,[d] Ti (5.894), Nb (0.011), Cl (0.445), 85.383%	Antioxidant, unknowns
Polyvinyl alcohol	PVOH-1	Sigma Aldrich	$M_w \sim 31$ kDa	17.6, 1.5	30	176.3, 22.9%	C (53.93), H (8.83), F (0.10), B (0.026),[d] Na (0.221), Si (0.268), Ti (0.005), 63. 380%	UV-absorber, unknowns
	PVOH-2	Sigma Aldrich, 81365 – 250 g, BCCD4007	$M_w \sim 130$ kDa flakes, colorless Mowiol®18-88	48.4, 1.3	41	173.6, 25.0%	C (53.72), H (8.81), F (0.10), B (0.023),[d] Na (0.099), Si (0.217), Ti (0.005), 62.974%	Minimal additives
	PVOH-3	Sigma Aldrich, 324590 – 500 g, STBJ9088	Average $M_w \sim 205$ kDa flakes, colorless, Mowiol®40-88	71.7, 1.4	42	171.1, 23.4%	C (53.71), H (8.77), F (0.16), B (0.025),[d] Na (0.077), Si (0.218), Ti (0.006), 62.966%	BTEX, unknowns
Ethylene vinyl alcohol	EVOH-1	Soarnol, DT2904	29 mol% ethylene pellets, colorless, ≤0.30% volatile matter, T_g 62 °C, T_c 163 °C	21.8, 1.5	46	184.5, 35.3%	C (60.96), H (10.31), F (0.78), B (0.032),[d] Na (0.026), Cl (0.009), 72.117%	Phthalates
	EVOH-2	Sigma Aldrich, 414093 – 100 g, MKCP5380	32 mol% ethylene pellets, colorless	18.4, 1.5	49	179.7, 40.1%	C (61.07), H (10.53), F (0.10), B (0.024),[d] Na (0.050), Ca,[d] 71.774%	Unknowns
	EVOH-3	Soarnol, DC3203	32 mol% ethylene pellets, colorless, ≤0.30% volatile matter, T_g 61 °C, T_c 160 °C	19.9, 1.4	45	178.4, 36.8%	C (61.08), H (10.35), B (0.036),[d] Na (0.019) Ca,[d] 71.485%	Monomer, phthalates
	EVOH-4	Soarnol, ET3803	38 mol% ethylene pellets, colorless, ≤0.30% volatile matter, T_g 58 °C, T_c 152 °C	18.4, 1.5	48	168.8, 33.8%	C (62.73), H (10.61), F (0.10), B (0.047),[d] Na (0.025), Ca,[d] 73.512%	Monomer, phthalates, slip agents
	EVOH-5	Soarnol, AT4403	44 mol% ethylene pellets, colorless, ≤0.30% volatile matter, T_g 55 °C, T_c 164 °C	21.0, 1.4	48	160.5, 32.3%	C (63.98), H (10.81), F (0.16), B (0.048),[d] Na (0.017), Cl (0.014), 75.029%	Monomer, phthalates, slip agents
Polylactic acid	PLA-1	Goodfellow, ME346310/4	Biopolymer granule, nominal granule size 3–5 mm, melt flow rate 6	173.8, 1.6	50, 61	150.1	C (50.13), H (5.96), B (0.016),[d] Si (0.014), Cl (0.062), 56.182%	Monomer, phthalates, unknowns
Polyacrylo-nitrile	PAN-1	Goodfellow, AN316010/7	Powder, mean particle size 500 μm, co-polymer 99.5% acrylonitrile, 0.5% methyl methacrylate, M_w 230 kDa, 0.1% S, <10 mg kg^{-1} Cl, 230–400 mg kg^{-1} K, 100–230 mg kg^{-1} Na, <2.5 mg kg^{-1} Fe, T_g 80–90 °C	214.6, 2.4	—	—	C (67.07), H (6.16), N (26.12), F (0.33), B (0.026),[d] Na (0.022), Si (0.251), Ti (0.006), 99.985%	Antioxidant, unknowns

Table 1 *(Contd.)*

Polymer type	Sample code	Supplier, product number, lot number	Supplier description	M_w (kDa), $Đ$	T_g (°C)[a,b]	T_m (°C), % crystallinity[c]	CHNS, F, and ICP-MS elemental composition (wt%), total wt%	Probable extractable additives
Polybutylene terephthalate	PBT-1	Goodfellow, ES341050	Film (0.55 mm)	45.1, 1.9	52	229.7, 32.1%	C (65.12), H (5.83), S (0.16), F (0.10), B (0.024),[d] Si (0.171), Ti (0.010), 71.415%	Minimal additives
Polyketone	PK-1	Goodfellow, PK306310/1	Granule, nominal granule size 3–5 mm, natural color, low viscosity	56.5, 1.8	—	220.5	C (64.41), H (7.61), B (0.026),[d] 72.004%	Plasticizer, UV-absorber
Polyhydroxy butyrate	PHB-1	Goodfellow, BU396311/9	Biopolymer granule, nominal granule size 5 mm, M_w 550 kg mol^{-1}, green production, Biomer® P226 Grade	714.7, 5.3	52	173.5, 44.1%	C (56.65), H (7.54), N (0.21), S (0.12), F (0.20), B (0.108),[d] Si (0.042), 64.870%	Plasticizers, unknowns
Styrene acrylonitrile	SAN-1	Scientific Polymer Products, 82	20% acrylonitrile	232.0, 2.1	77[a]	103.6	C (84.41), H (7.30), N (7.58), S (0.26), F (0.10), B (0.036)[d], Si (0.064), 99.750%	Monomers, UV-absorber, many unknowns

[a] DSC measurement reported from the cryomilled substrate. [b] DSC measurement taken from second heating cycle. [c] Recorded melting temperature unrelated to polymer backbone. [d] Boron was semi-quantified using a separate method. Ca values were not reported but recorded as present when above three times the analysis blank.

widely available vendors and to thoroughly characterize new polymer substrates to enable direct comparison between studies.[1,28–33] As part of the characterization portfolio, it is essential to report the polymer chemical composition (*e.g.*, monomer identities, additives), and physical properties (*e.g.*, molecular mass distribution, thermal properties). Structural and thermal properties of polymers as well as inorganic and organic additives may contribute to how polymers behave both physically and chemically in recycling processes.[34,35] Here we analyzed 59 polymers, all of which were commercially available, with varying levels of descriptions and quality control reports. Examples of commonly included information from vendors were average molecular mass, particle size, and copolymer composition (*e.g.*, % vinyl acetate in polyvinyl acetate). Information about possible additives present was provided for 6 plastics, 2 of which were not specific (*e.g.*, % total volatiles). All information provided by commercial vendors is included in Table 1, alongside our characterization data, in the language provided by the vendor.

These 59 polymers were characterized using methods as described in detail in the Experimental section, which is summarized here. To investigate the presence of organic additives, we conducted accelerated solvent extraction (ASE) followed by gas chromatography-mass spectrometry (GC-MS), pyrolysis GC-MS (PyGC-MS), and high-resolution GC-MS (HRGC-MS). Bulk characterization included carbon, hydrogen, nitrogen, and sulfur (CHNS) quantification and elemental analysis by inductively coupled plasma mass spectrometry (ICP-MS), which provided evidence of inorganic content. We characterized molecular composition and polymer morphology using Fourier-transform infrared spectroscopy (FTIR), gel permeation chromatography (GPC), and small-angle and wide-angle X-ray scattering (SAXS, WAXS). Thermal properties were measured using differential scanning calorimetry (DSC), and thermal gravimetric analysis (TGA). For the 21 polymers with TGA weight loss events >1% before the onset of polymer degradation, we conducted evolved gas analysis (EGA) with a TGA-FTIR, which provided insight into polymer structure as well as the presence of small molecules. We also investigated changes in structural properties pre- and post-cryomilling, which is a common preprocessing technique in recycling studies where plastics are size-reduced by grinding or milling the plastic at cryogenic temperatures (−150 °C).

The ESI contains all data referenced in the manuscript. In the main text, we present results which illustrate both the importance and respective limitations of each characterization technique. We included a secondary ESI file† that contains a summary of all the data generated, and raw data files in this work can be accessed on the data repository website Figshare.com titled "BOTTLE Plastic Substrates Database". The purpose of this database is to ensure the accessibility of fully characterized plastic substrates to the broader research community. We acknowledge that certain characteristics will likely change between lot numbers, and therefore the data presented in this study reflect values for a specific lot number and may not reflect different lot numbers from the same product number.

Organic additives by mass spectrometry

Mass spectrometry is an important tool in the identification of specific compounds used as additives in plastics.[18,36,37] In this study, samples were screened for organic additives using accelerated solvent extraction (ASE) and gas chromatography-mass spectrometry (GC-MS), and separately by pyrolysis GC-MS (PyGC-MS), with a list of example organic additives in Table 2. These compounds were tentatively identified using NIST and F-Search (Frontier Laboratories) library matching and have not been confirmed by standards. In the following section, we will describe the potential additives observed using these methods, as well as the limitations of these techniques.

Several polymers had observable excess monomer content *via* ASE GC-MS, including caprolactam (nylon-6), methyl methacrylate (PMMA), and 3,6-dimethyl-1,4-dioxane-2,5-dione (PLA). 3-[1-(4-Cyano-1,2,3,4-tetrahydronaphthyl)]propanenitrile and other isomers were an observed monomer mixture in SAN and all ABS substrates.[38] Monomers were also observed by PyGC-MS in SAN, including 2-propenenitrile and styrene, which is consistent with the literature.[39] The compound 1,3-butadiene, was observed in PBT-1 by PyGC-MS, but not by ASE GC-MS because 1,3-butadiene is a dehydration product of PBT.[40] Crotonic acid, isocrotonic acid, and 2-butenedioic acid, all known PHB degradation products, were observed in the PyGC-MS of PHB-1, highlighting how this technique has the capability to release compounds from the backbone of the polymer.[41–43]

Slip agents and lubricants are employed in pre- and post-processing. For example, wax mixtures can be used as a processing aid, or to impart characteristics to the plastic such as color consistency and mechanical integrity.[19] We observed that many polymers contained wax-like mixtures, as well as individual slip agent components. All PP samples tested contained wax mixtures, as well as 8 of the 9 PE samples (excluding PE-9). Several polymers contained individual slip agents such as palmitic acid, ethyl palmitate, and oleic acid. Many of these wax mixtures were not observed using PyGC-MS. This is likely because a larger volume of sample was extracted using ASE *vs.* PyGC-MS (500–1000 mg *vs.* 1 mg, respectively).

Even though plasticizers, primarily in the form of phthalates (*e.g.* diethyl phthalate, benzyl butyl phthalate, di(2-propylpentyl) ester phthalic acid, *etc.*) are often associated with PVC, they were found in 25 plastics, whereas stabilizers, UV-absorbers, and antioxidants were observed in 11 polymers (Table 2). These compounds are likely related to hydroxybenzophenones, benzotriazoles, and organophosphorus compounds. Butylated hydroxytoluene (BHT) was the most frequently observed antioxidant, including in all 3 EVA plastics, which were noted in the certificate of analysis for EVA-1 and EVA-2 from Sigma-Aldrich at concentrations of 527 ppm and 470 ppm, respectively. EVA-3 did not have a quality report with information on BHT concentration. PP-7 likely contains a phosphite-based stabilizer, which is supported by a measurable amount of phosphorus by ICP-MS (*vide infra*). The library match was 79.2% for tris(2,4-di-*tert*-butylphenyl) phosphite, which is too low of a match to be considered tentatively identified (>85%), but it is likely a related structure to what is present. Drometrizole, a common UV-absorber used in acrylates due to its environmental stability, was observed in PMMA 4–6.[44] One sample, PE-2 from NIST (SRM-1475) was analyzed in 1971 with a report indicating the presence of antioxidant Irganox 1010. While this polymer is no longer produced, and has recently been discontinued in distribution, it has been used since 1971 as a standard reference material,[45] including in a recent PE depolymerization study from 2021, and a Google Scholar search of "SRM-1475" resulted in 235 matching studies.[46] For PE-2 (SRM-1475), ASE GC-MS results also indicated the presence of many other compounds including a wax mixture, diethyl phthalate, and tridecanoic acid (Fig. S1 and Table S1†).

Table 2 Additive classes observed in this study, with example chemical structures, as well as a list of polymers that likely contain these types of additives. Organic additives were measured using ASE GC-MS and PyGC-MS. Polymers possibly containing fillers were not listed because there is only indirect measurement of elements that might indicate the presence of fillers

Additive class	Tentatively identified observed examples	Polymers
Process aids (slip agents, lubricants, wax mixtures, co-polymers)	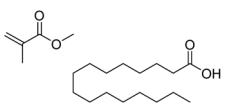	PE-(1–11), PP-(1–7), PVC-(1–2), PS-(1–5) ABS-(1–3), nylon-6, nylon-66, PMMA-(1–6), PC-1, PVAc-1, EVA-(1–3), EVOH-(1–5), PLA-1, PK-1, PHB-1, SAN-1
Stabilizers (UV-absorbers, antioxidants)	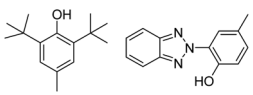	PE-(2,5,6,11), PP-(1,3,4,7), PVC-2, PU-1, ABS-1, PMMA-(1,3–6), PC-1, EVA-(1–3), PVOH-1, PAN-1, PK-1, SAN-1
Plasticizers (phthalates, citrates)	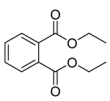	PE-(2,5,6,9,11), PET-(2,3), PP-(4,6) PVC-(1,2), PS-2, PU-1, ABS-(1–3), nylon-66, PMMA-(2–6), PC-1, PVAc-1, EVA-1, EVOH-(3–5) PLA-1, PK-1, PHB-1
Colorants (pigments, dyes)	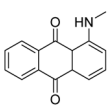	PVC-(1,2), ABS-(1–3), nylon-6, nylon-66, PMMA-(1,2,4–6), PC-1, EVA-3, PVOH-(1–3), PAN-1, PBT-1
Flame retardants (organo-phosphorus compounds, inorganics)	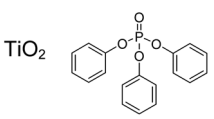 TiO_2	PVC-2, EVOH-4, PMMA-(1,2) PLA-1; likely in polymers containing B, Al, P, Mg, Zn, or Al
Fillers	$CaCO_3$	Likely in polymers containing: Ca, Si

PMMA-4, PMMA-5, and PMMA-6 contained red, blue, and green dye compounds respectively. 1-(Methylamino)anthraquinone, otherwise known as disperse red 9, was the only observable dye by ASE GC-MS. Many dyes do not ionize with electron ionization (EI) and are unlikely to be detected by GC-EI-MS directly. Other techniques, such as liquid chromatography-MS would need to be utilized to target these types of compounds, as well as other non-volatile or larger molecular weight compounds.

There are benefits and limitations to both ASE GC-MS and PyGC-MS. Compounds that are more integrated into the polymer are less likely observed by ASE GC-MS, as they are more difficult to extract. This can be highlighted by PBT-1, which had no observable extractables, but many observable compounds by PyGC-MS (Fig. S2†). PyGC-MS is also useful in situations where there is limited sample quantity, such as microplastics from the environment, whereas ASE extraction is more sensitive for extractables because of higher sample volumes. This was observed with wax mixtures in many PE and PP samples (Fig. 2). Cryomilling likely improves extraction efficiency and can potentially release integrated additives.[47] Many polymers contained unknown compounds not identified by the NIST or F-Search libraries. Conducting structural analysis for unknown plastic additives would require advanced analytical techniques such as high-resolution mass spectrometry, and/or fractionation with NMR spectroscopy. In this work, we collected high-resolution GC-MS mass spectra for unknowns found in all PE, PP, PET, and PS, which are included in the online Figshare database for future analyses. To our knowledge, there were only four reports of a commercial vendor providing specific additive information in this study (PE-2, PS-2, EVA-1, and EVA-2).

Elemental analysis

Elemental analysis is useful for determining the chemical composition of a polymer, the presence of inorganic components, and for confirming the chemical composition of organic additives. We conducted CHNS analysis and a 68-element screen on all plastic substrates (Table 1 and Fig. 3). We report elements that were measured at >0.005 wt% and note elements that are present in trace amounts (<0.004 wt%) in Fig. S1.† Without targeted analysis of specific inorganic additives, we could only make inferences about the possible additives present, given the specific elements present. For example, when characterizing an unknown polymer, the presence of aluminum could be from flame retardants such as aluminum hydroxide, or from an aluminum barrier layer. The following section discusses the possible presence of different classes of inorganic or organic compounds in these polymers given the presence of certain elements, which includes flame retardants, fillers, metals, and halogens.

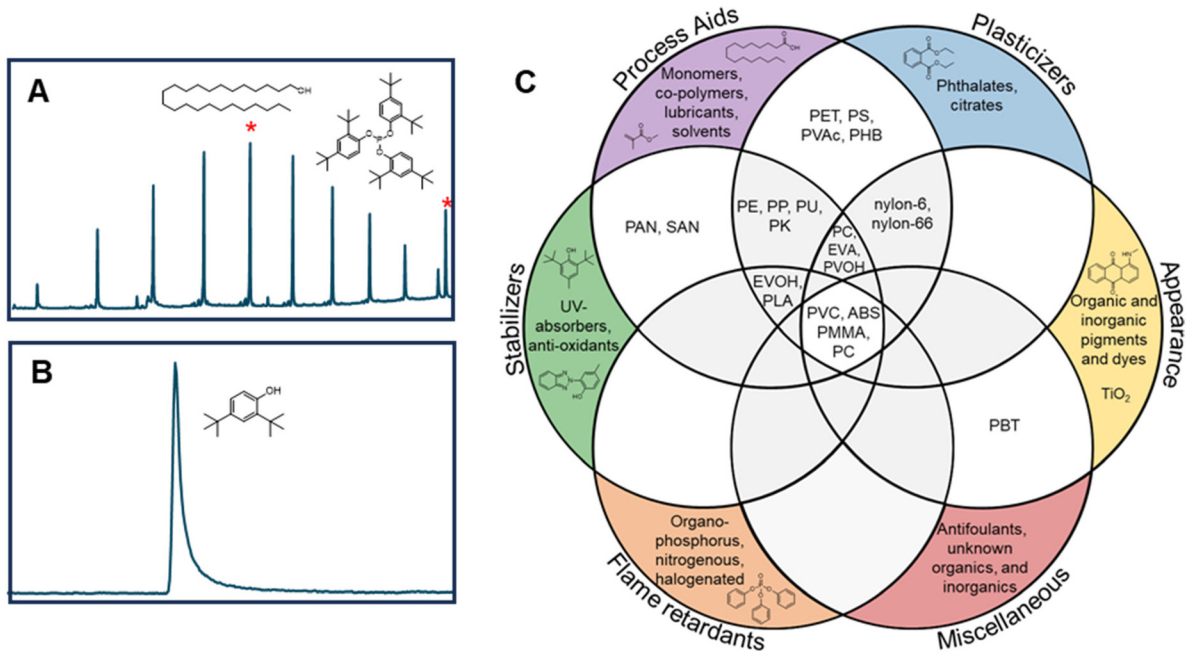

Fig. 2 (A) ASE GC-MS chromatogram of PE-6 that contains a tentatively identified mixture of fatty alcohols (*n*-tetracosanol-1 highlighted), tris(2,4-di-*tert*-butylphenyl) phosphite (Alkanox 240), and 2,4-di-*tert*-butylphenol, as well as unknowns. (B) PyGC-MS chromatogram of PE-6 contains tentatively identified 2,4-di-*tert*-butylphenol. These results highlight how these two techniques, ASE GC-MS and PyGC-MS complement each other by targeting extractable additives *vs.* additives that are more tightly bound to the polymer. (C) A Venn diagram with polymer class separated by the types of tentatively identified additives present from stabilizers, process aids, plasticizers, flame retardants and appearance compounds, highlighting that most polymers contain several different classes of additives.

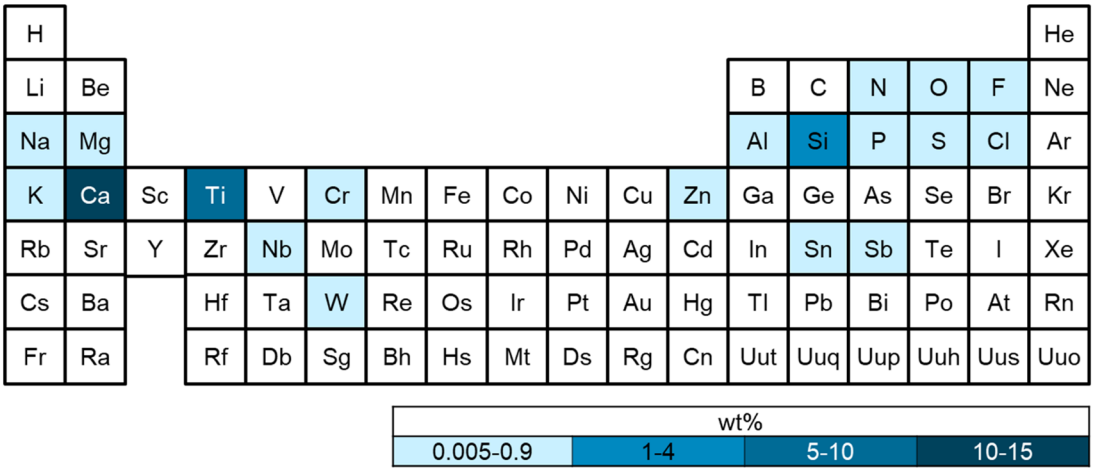

Fig. 3 Periodic table of highest weight percent concentrations of elements measured in 59 plastic samples. These results indicate that most research grade polymers contain additives with inorganic content. The elements found at the highest concentration included Ca, Ti, and Si. For most elements, samples were digested using microwave acid wet digestion (MAWD), and then analyzed using inductively coupled plasma mass spectrometry (ICP-MS). Fluorine was analyzed potentiometrically following combustion.

Some polymers that did not contain nitrogen in the polymer backbone contained an appreciable amount of nitrogen, including EVA-3 (0.9 wt%), PP-4 (0.2 wt%), and PHB-1 (0.2 wt%). It is possible that this nitrogen originates from additives or processing aids. GC-MS data indicates that there are several unknown additives in each of these polymers, which may contain nitrogen. PHB is a bio-derived plastic, and therefore the nitrogen may be from residual media or cellular material.

Some polymers exhibited a sulfur content between 0.1–0.8 wt% (Table S2†). Elemental sulfur is sometimes added to plastics as a processing aid or stabilizer, and sulfur-containing organic additives can be used as chain transfer agents, stabilizers, plasticizers, processing aids, and curing agents including mercaptans, thiurams, dithiocarbamates,[48] thioureas,[49] and thiols.[48–51] PMMA-2 contained 0.1% S, and had GC-MS library matches for 1-dodecanethiol and *N*-ethyl-2-methyl-benzenesulfonamide (EMBSA). The addition of 1-dodecanethiol can improve surface properties which can help to reduce the adhesion of contaminants due to its high hydrophobicity.[52] EMBSA can also be used as a plasticizer, a modifying agent in PMMA, and a component of ink formulations.[53,54] While there is evidence of the source of sulfur in PMMA-2, the source of sulfur in nylon-66, EVA-3, and several PE samples is unknown.

Flame retardants are another common class of polymer additives, and often contain inorganic elements such as boron (borates, boron oxide), aluminum (aluminum trihydrate), phosphorus (organo-phosphates, phosphonates), antimony (antimony trioxide), magnesium (magnesium hydrate), and zinc (zinc borate).[55,56] Aluminum was detected in 13 plastics (0.005–0.413 wt%), 51 contained boron (0.014–0.108 wt%). While boron and aluminum-containing compounds can be used as flame retardants and heat stabilizers,[57,58] boron can also act as a nucleating agent, and aluminum is commonly used as a barrier material.[59,60] It is unlikely the polymers in this study contained an aluminum barrier, which is commonly used in plastic films such as multi-layer food packaging. Phosphorous was observed in 3 polymers (0.005–0.028 wt%), while 4 contained antimony (0.008–0.063 wt%). Phosphorous-containing additives are almost always organic and can be used as flame retardants and stabilizers, while antimony is also used as a catalyst in the production of PET.[55,56,61] All three PET polymers contained antimony, which is likely from the polymerization catalyst antimony trioxide (Sb_2O_3). Magnesium was observed in 6 polymers (0.005–0.081 wt%), and 6 contained zinc (0.006–0.011 wt%). Polymers that contain both zinc and boron may contain zinc borate, a commonly used flame retardant. Zinc-containing compounds can also be used as thermal stabilizers, slip agents, fillers, and to prevent discoloration (*e.g.*, zinc oxide and zinc stearate).[13,62] Other salts that were observed included sodium and potassium (0.005–0.100%).

Fillers are commonly used to improve performance, processing, and costs of polymers. Silica or silicon dioxide, and calcium carbonate are both common reinforcing fillers, as well as zinc oxide, metal, and wood powders.[19] Calcium and silicon exhibited a high laboratory background but were observable above blank concentrations in 30 plastics. In one study, it was found that single-use plastic bags contained 15–36 wt% inorganic additives primarily as calcium carbonate ($CaCO_3$) and titanium dioxide (TiO_2).[20] Titanium was measured in 20 plastics (0.005–5.894 wt%), likely from TiO_2. Inorganic pigments can be up to 10 wt% in plastics, with TiO_2 accounting for approximately 70% of total pigment volume globally.[63]

Several plastics contained small amounts of certain metals. Chromium (Cr) was found in 2 plastics (0.005–0.012 wt%), 1 with niobium (Nb) (0.011), 1 with tin (Sn) (0.380), and 2 with tungsten (W) (0.005–0.07). While Cr is used as a filler, colorant, and corrosion inhibitor, its use is likely limited because of

environmental regulations on hexavalent chromium.[64] Tin oxide (SnO_2) and tungsten oxide (WO_3) can be used as catalysts, or as fillers to improve properties such as barrier resistance or hardness.[19] Niobium is rarely used in plastic, but could be excess catalyst or from an additive such as niobium oxide (Nb_2O_5), which increases polymer hardness.[65]

Measurable amounts of fluorine were found in 38 plastics (0.1–0.8 wt%), and likely derives from fluorinated additives. Low molecular weight polytetrafluoroethylene (PTFE) powders are largely consumed by industries outside of fluoropolymers, where fluorinated coatings and additives are generally used to impart specific properties such as lower water permeability.[66] These types of fluorinated compounds are typically measured using LC-MS, which was not conducted for this study. Beyond PVC, which contains chlorine in the polymer backbone, chlorine was found in 9 plastics (0.009–0.005 wt%). Several classes of plastic additives contain chlorine, including chlorinated paraffins, which are used as plasticizers or flame retardants, and chlorinated isocyanurates, which are used as antimicrobial agents.[19,67]

All elements highlighted in Fig. S3† (*e.g.*, lanthanides, radionuclides, transition metals) were observed at trace levels (≪0.004 wt%). These are all likely contaminants introduced during plastic processing, or possibly trace amounts of excess catalyst. These elemental concentrations are likely naturally occurring and were measured significantly below toxic levels.[68]

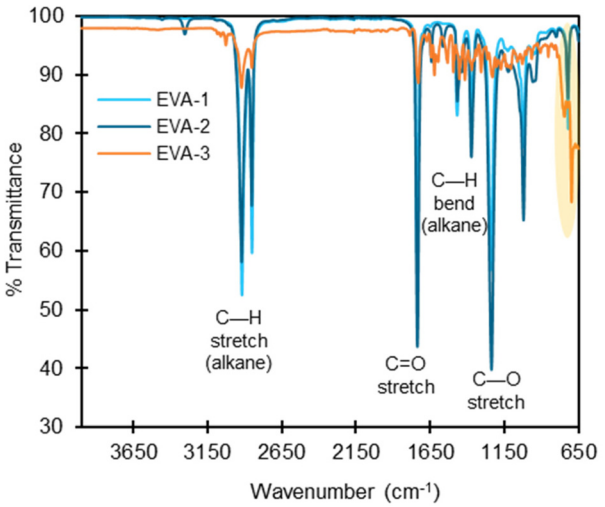

Fig. 4 FTIR spectra overlay of EVA-1, EVA-2, and EVA-3 with labeled absorbance bands. Most polymer classes have nearly identical FTIR spectra, indicating minimal structural differences (Fig. S2–S20†). EVA-3 has clear differences in the intensity of absorbance bands at the C—H stretch, C=O stretch, C—H bend, and C—O stretch regions (labeled). There are also absorbance bands in regions not shared by EVA-1 and EVA-2, including in the C–Cl stretch region of 550–850 cm^{-1} (highlighted in yellow). This indicates possible differences in structure and/or the presence of additives.

Structural and thermal analysis

Fourier-transform infrared (FTIR) spectroscopy

FTIR spectroscopy is a characterization technique that provides information about the bonding topology in the bulk polymer. We overlaid the FTIR spectra for each polymer class containing more than one studied substrate (Fig. S4–S14†), and in most cases for polymer types with multiple substrates, all polymers within a class exhibited similar spectral patterns.

Deviations in the FTIR spectra can be used to detect the presence of additives or co-polymers. In the current work, EVA-3 exhibited signals in the 1700–650 cm^{-1} range that were significantly different from the other two commercial EVA polymers (Fig. 4). The extra signals possibly indicate the presence of additives or other co-polymers. The GC-MS chromatogram after ASE extraction of EVA-3 presented multiple unknown structures that possibly contain C=C bonds, which could explain the peaks in the 1400–1600 cm^{-1} region. We also measured 0.4 wt% of sulfur, indicating the presence of either elemental sulfur, inorganic, or organosulfur compounds, and there are peaks in the 1070–1030, 1370–1300, 1415–1380, and 1195–1168 cm^{-1} regions, which could be attributed to S=O stretching. EVA-3 also contained peaks between 3250–3000 cm^{-1}, which is either from C–H alkene stretching or O–H stretching. Notably, there are signals in the C–Cl region (550–850 cm^{-1}), and Cl was measured at 0.445 wt% in EVA-3. While FTIR is not sufficiently sensitive to detect or distinguish low concentrations of additives, it is a valuable tool for rapid, bulk characterization of polymers.

Thermogravimetric analysis (TGA) and evolved gas analysis (EGA) using TGA-FTIR

TGA measures weight changes in a material as a function of temperature. For polymers, TGA provides the degradation temperature of the polymer and can indicate the presence of volatiles, water, small molecules, additives, and/or additional polymers. TGA and EGA using TGA-FTIR can be used to identify additives either by determining remaining residue at 800 °C or by monitoring the FTIR spectra of the evolved gas. We first conducted TGA for all polymer substrates under nitrogen. Weight loss events >1 wt% before the onset temperature of polymer degradation occurred in 21 of 59 plastic samples (Tables S3–7†), suggesting the presence of organics that can evaporate or desorb from the polymer. In all of the TGA experiments under air, we attribute any remaining residue above 800 °C likely to be inorganic material, such as salts, metal oxides, or recalcitrant carbonaceous material.[69]

Polymers with >1 wt% residue under nitrogen TGA experiments included PVC-2 (32 wt%), EVA-3 (18 wt%), PC (20 wt%), PET-1 (9 wt%), PET-2 (10 wt%), PET-3 (11 wt%), PBT (5 wt%), and PK (19 wt%). We then analyzed these polymers under air (21% oxygen) to 900 °C, which reduced the residue wt% for all polymers (except EVA-3 and PVC-2) to <0.3 wt%, indicating that these weight loss events are likely from carbonaceous material. PAN also had a high residue (34%), which we attribute to a known cyclization reaction PAN undergoes in the

absence of oxygen by a free radical mechanism resulting in the formation of carbon fibers.[70] This explains why the high residues observed for PAN-1 under nitrogen were subsequently reduced under air (34 wt% to <0.3 wt%).[70] Under an air environment, EVA-3 and PVC-2 had residual wt%s of 11% and 8% respectively (Fig. 5), which indicates they likely have high oxidative stability because they contain relatively high amounts of flame retardant materials, possibly including organic and inorganic additives.[71] This is consistent with ICP-MS results, which indicate signifcant concentrations of Ti in EVA-3 and PVC-2 (5.894 wt% and 3.865% respectively).

EGA using TGA-FTIR was performed on 21 polymers which had >1 wt% loss events before the polymer degradation temperature in an inert environment to investigate the presence of additives, with selected examples shown in Fig. 6. Table S8 in the ESI† includes the FTIR vapor phase library matching results for EGA analysis of TGA polymer mass loss events for all 21 polymers, which includes the onset temperature of each mass loss event and total wt% loss for each degradation event. Many library matches are monomers or expected decomposition products of the polymer, including, for example, alkanes from PE; hydrogen chloride, benzene, and 1-chlorooctane from PVC; styrene from PS; acetic acid or acetaldehyde from PVAc, PVOH, EVA, and EVOH; and methyl methacrylate from PMMA (Fig. 4). Multiple weight loss events for PMMA samples had FTIR spectral library matches for methyl methacrylate, indicating either lower molecular mass polymer with lower thermal stability, or excess monomer.

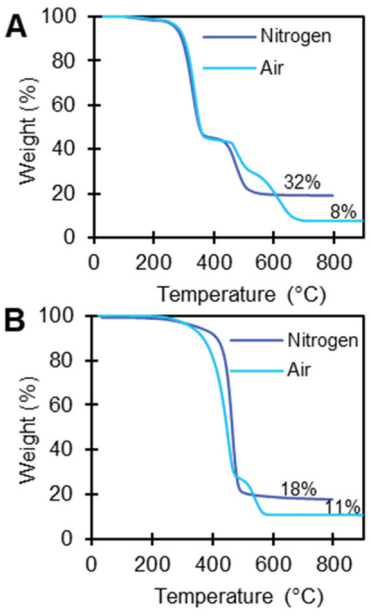

Fig. 5 TGA curves for (A) PVC-2 and (B) EVA-3 under nitrogen and air environments. PVC-2 exhibited a residue of 32 wt% under nitrogen, and 11% under air. EVA-3 had a residue of 18% under nitrogen, and 11% under air. This suggests that these two polymers contain flame retardants, either as organic or inorganic additives. Under nitrogen, samples were run from 35 °C to 200 °C at 4 °C min^{-1} and then 200 °C to 800 °C at 20 °C min^{-1}. Experiments with air were conducted from 30 °C to 900 °C at 20 °C min^{-1}.

EGA using TGA-FTIR (Table S8†) was able to clearly identify known or expected additives and/or processing aids in PE-2, PVC-2, PS-1, PU-1, and EVA-3 (Fig. 6). PE-2 exhibited a 1 wt% library match to butylated hydroxytoluene (BHT), which is a commonly used antioxidant that scavenges free radicals and other reactive species that cause polymer degradation.[72] There was a 1% weight loss event in PVC-2 that library matched 5-norbornene-2,3-dicarboxylic anhydride (NBDCA). NBDCA is used as a monomer in norbornene-based polymers, which are used as reactive processing additives in plastic manufacturing to improve the processing characteristics and physical properties of the final plastic product.[73,74] PS-2 exhibited a 97% library match for pentane at approximately a 2 wt% mass loss event, in agreement with information provided by the vendor. Here, pentane could have been used as a blowing agent in plastics to produce a lightweight, porous material.[75] PU-1 exhibited a library match for 1,2-dibutoxyethane with a significant weight loss (45 wt%). Even though, 1,2-dibutoxyethane can be used as a solvent or co-solvent in the production of certain types of plastic, including PU, the products detected here are likely from the thermal degradation of the polymer itself. As polyurethanes are extremely complex and made with many different formulations, this data highlights the potential to use EGA using TGA-FTIR for some product characterization.[76] Although EGA with TGA-FTIR may provide insight into the structure of this polymer, this technique alone cannot distinguish between a thermal degradation product or a small molecule additive. The FTIR spectra for EVA-3 exhibited a 77% library match for vinylbenzene and 3-methyl-1-phenyl-3-pentanol, indicating the presence of aromatic structures.

While TGA and TGA-FTIR provides valuable information on thermal stability, chemical structure, and the presence of additives, it is important to consider the limitations of these methods. FTIR library matches provide tentatively identified compounds as likely or similar structures, but matrix effects from strongly absorbing backgrounds or simultaneously evolving gases can interfere with spectral resolution and library matching. Additionally, in some cases, the library matching software cannot distinguish certain chemicals. For example, vapor phase FTIR library matching cannot distinguish nonadecanenitrile from other long-chain hydrocarbons due to nearly identical FTIR spectra. Several polymers had a library match for nonadecanenitrile and other long-chain hydrocarbons including PVAc (22 wt%), EVA-1 (77 wt%), and EVA-2 (70 wt%) (Table S8†). As neither PVAc, EVA-1, or EVA-2 contained a measurable amount of nitrogen based on CHN analysis (>0.1 wt%), they are unlikely to contain such a high amount of nonadecanenitrile, and likely contain hydrocarbons. While this is an obvious case, it is more difficult to distinguish library matches when characterizing unknown or mixed materials. Instruments such as TGA GC-MS may be useful to further resolve these issues. Instrumental sensitivity is also a limitation of TGA and TGA-FTIR, with detection limits generally around 1 wt%, while many additives can be present at

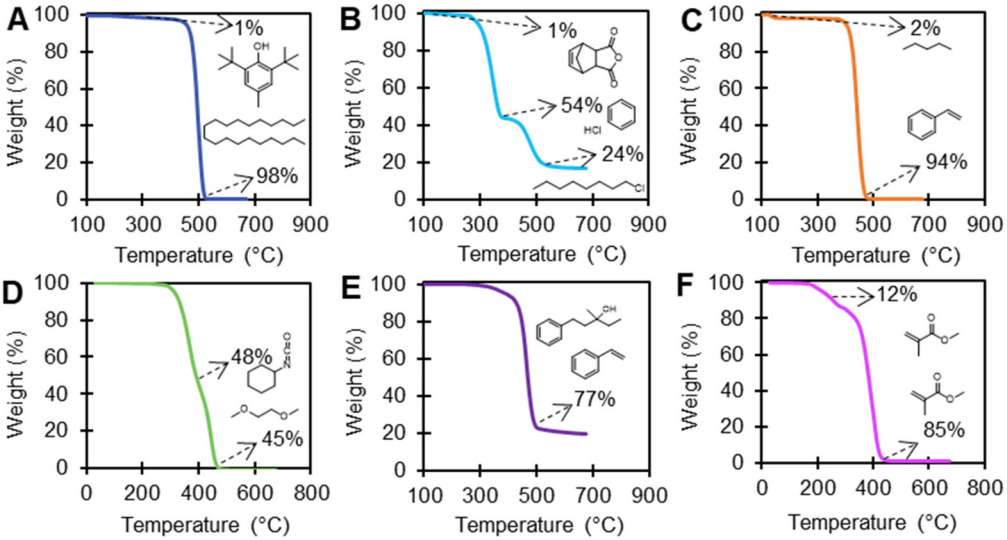

Fig. 6 TGA traces from TGA-FTIR with EGA for several polymers with tentatively identified products. (A) PE-2 exhibited weight loss events of 1 wt% butylhydroxytoluene and 98 wt% alkanes, with a representative compound shown. (B) PVC-2 displayed a weight loss of 2 wt% 5-norbornene-2,3-dicarboxylic anhydride, 54 wt% HCl and benzene, and 24 wt% 1-chlorooctane. (C) PS-2 showed weight loss events of 2 wt% pentane and 94 wt% styrene. (D) PU-1 exhibited weight loss events of 48 wt% cyclohexyl isocyanic acid and 45 wt%, of 1,2-dibutoxyethane. (E) EVA-3 displayed weight loss events of 77 wt% styrene and 3-methyl-1-phenyl-3-pentanol. (F) PMMA-1 which had two weight loss events of methyl methacrylate at 12% and 85%. TGA-FTIR can provide information on thermal stability, structural insight, and indicate the presence of additives above 1 wt%.

lower concentrations. This highlights the importance of using multiple techniques to characterize the chemical composition of polymers, including ICP-MS and mass spectrometry.

Gel permeation chromatography (GPC)

Molecular mass distributions are critical polymer characteristics that impact multiple properties[77] as well as polymer solubility in solvents.[78] Moreover, molecular mass and dispersity of polymers can impact yields and speciation of products depending on the recycling technology.[79,80] Accordingly, GPC was used to measure the weight-average molecular mass (M_w), number-average molecular mass (M_n), and dispersity ($Đ$) of the 59 polymers analyzed here. Since different polymer classes are soluble in different solvents, each polymer required specific conditions for GPC. For this study, two types of GPC systems were used including (1) a GPC system with dual multi-angle light scattering (MALS) and differential refractive index (dRI) detectors and (2) a high temperature GPC (HT-GPC) with a dRI detector. When possible, the system with both MALS and dRI detectors were used, because a MALS detector allows for the absolute measurement of M_w. Several polymer classes including PE, PP, and EVA required the use of HT-GPC to solubilize the polymer, despite the lack of a MALS detector. Table S11† lists the GPC conditions for each polymer class used in the study including solvents, columns, and detectors. In this section, we present important results and discuss several limitations of GPC.

Once analyzed, we compared the molecular masses to those reported by suppliers. Many suppliers only provide a single number, which we found more likely to correlate with M_w. Additionally, most molar mass distributions were broad, which was not reported by suppliers. For example, PS-5 was reported to be 35 kDa (M_w) by the supplier but the $Đ$ was not provided. GPC results for PS-5 indicate that it has a bimodal molecular mass distribution with an M_w at approximately 35 kDa across both distributions (Fig. 7). Several other polymers were found to exhibit bimodal molecular mass distributions including PBT-1, PET-2, PET-3, and PVC-2 (Fig. S15†).

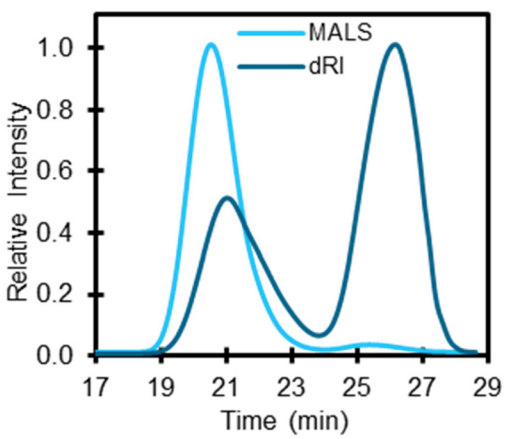

Fig. 7 GPC trace for PS-5 using a multi-angle light scattering (MALS) and a differential refractive index (dRI) detector. Retention times 21 min (M_w 113.6 kDa) and 26 min (M_w 1.8 kDa) show two unique molecular mass distributions. Other GPC traces for bimodal polymers can be found in Fig. S15.† While MALS is not affected by non-ideal column interactions, dRI can provide relative concentration of molecular mass distributions. The operating conditions included using THF as the mobile phase, a flow rate of 1.0 mL min^{-1}, column oven temperature set to 40 °C, and a sample injection of 100 µL.

One benefit of using a concentration detector, such as dRI, is that the change in refractive index is proportional to concentration and therefore can be used to estimate relative abundance of molecular masses. For example, PS-5 dRI (Fig. 7) shows that the first molecular mass distribution at 21 min (M_w 113.6 kDa) is 36% of the total mass percent and the second molecular mass distribution at 26 min (M_w 1.8 kDa) accounts for 64%.

There are limitations with using GPC to measure molecular mass. Without the use of a light scattering detector, size exclusion chromatography relates molecular mass with retention time assuming the analyte elutes in accordance with a calibration curve, most commonly PS. Analysis for non-PS materials can be improved by applying Mark–Houwink correction values to the PS calibration curve, which relate the relative residence times of two materials which behave differently in the same solvent. Use of a viscometer to derive Mark–Houwink correction values can also enable the correction of differences in residece times for two polymers from the same class, but with different architectures. Mark–Houwink values used in this study can be found in Text S3.† Retention times can shift with different solvents, and if there are non-ideal column interactions. This can result in erroneous calculations of molar mass when comparing to a calibration curve. For example, all PS samples were run separately on GPC with tetrahydrofuran and HT-GPC with trichlorobenzene and had 55–58% difference in molecular mass estimates. Alternatively, there was a 40–47% difference when using 100% mass recovery as opposed to using a literature value for differential index of refraction (dn/dc) (Table S9†). The dn/dc values represent the difference in refractive index between the sample and solvent, and are unique to sample-solvent combinations as well as instrumental conditions, including temperature and laser wavelength. While PS has literature dn/dc values that closely match our instrumental conditions, many polymer types do not for these conditions, including PE, PP, PU, PK, PLA, and PHB. Copolymers, such as PVOH, EVA, EVOH, PBT, ABS, and SAN pose an additional challenge because the dn/dc is related to the relative ratios of the different monomers, which varies from product to product. When possible, the optimal method to measure molecular mass is to determine dn/dc for each polymer with the specific instrumental conditions they will be measured in by injecting the analyte directly into a dRI detector at multiple concentrations. When this is not possible, multi-angle light scattering (MALS) should be used to estimate molecular mass assuming 100% mass recovery, as it depends on scattered light intensity and is not impacted by non-ideal column interactions or retention time.

Differential scanning calorimetry (DSC)

DSC determines the temperature and heat flow associated with material transitions as a function of temperature and time, and it can provide information on the glass transition temperature (T_g), melting temperature (T_m), crystallization temperature (T_c), cold crystallization temperature (T_{cc}), and percent crystallinity of polymers, all of which can be critical parameters for various recycling approaches. The presence of unusual endotherms and exotherms can also provide information on polymer structure or the presence of additives. In this section, we highlight interesting results and the limitations associated with DSC data interpretation.

T_g is an important parameter because it is when a polymer transitions to a softer, more pliable state, which will impact polymer behavior in recycling processes. Unlike melting, the observed T_g depends on the heating rate. We reported the T_g for all polymers where applicable in Table 1, and we note that, in many polymers, a glass transition was not detected using DSC. For polymers with high crystallinity (*e.g.*, PE, PK), the T_g is often difficult to detect by DSC, or was out of the temperature range of the instrument. Weak glass transitions can possibly be detected by increasing the ramp rate, or by using other techniques such as dynamic mechanical analysis.[81] Several polymers contained multiple T_g values, indicating a complex polymer morphology. For example, PP-2 exhibited two glass transitions (−12 °C, 51 °C) (Fig. 8). The lower T_g is attributed to a non-stereoregular amorphous region, or possibly oligomeric wax. Meanwhile, the higher T_g is attributed to the stereoregular portions of the polymer, a known phenomenon for PP.[82] In contrast, PP-1 had a simpler DSC trace, with only a T_m and T_c observed.

Another important parameter that can be measured by DSC is crystallinity, a measure of the ordered structure of a polymer relative to the disordered, amorphous regions. This property can impact polymer processability and the efficiency of various conversion processes. Percent crystallinity can be determined by comparing enthalpies of melting (ΔH_m) of a 100% crystalline polymer in literature to experimental values. This property can impact polymer processability and efficiency of various conversion processes. We calculated percent crystallinity for polymers with clear melting endotherms, and which had published ΔH_m for 100% crystalline polymer in literature (eqn (S1)†). These include PE, PP, PET, PVOH, EVOH, PVAc, PBT, PHB, nylon-6, and nylon-6,6 (Table 1). It is important to subtract the enthalpy of cold crystallization from the enthalpy of melting when determining percent crystallinity because this determines the crystallinity of the polymer before heating occurred during the DSC measurement. Polymers that exhibited melting points above our highest instrument temperatures or above the polymer degradation temperature could not be detected by DSC. These include most PS samples (except PS-5), PVC, ABS, PC, PU, PMMA, and PAN. We observed a cold crystallization peak (*i.e.*, crystallization exotherm between the T_g and T_m) in PET-3 and PLA-1 (Fig. S16 and S17†). We suspect PLA-1 exhibited enthalpic relaxation and cold crystallization simultaneously with the T_g, and thus the cold crystallization and the T_g were not reported (Fig. S17†).

Aside from melting and crystallization temperatures, other endotherms and exotherms may indicate curing, chemical reactions, water absorption, or the presence of additives. For example, nylons readily absorb ambient water, and therefore must be dried before DSC measurements.[83] When not dried, nylon-6 and nylon-6,6 both exhibited inconsistent endotherms

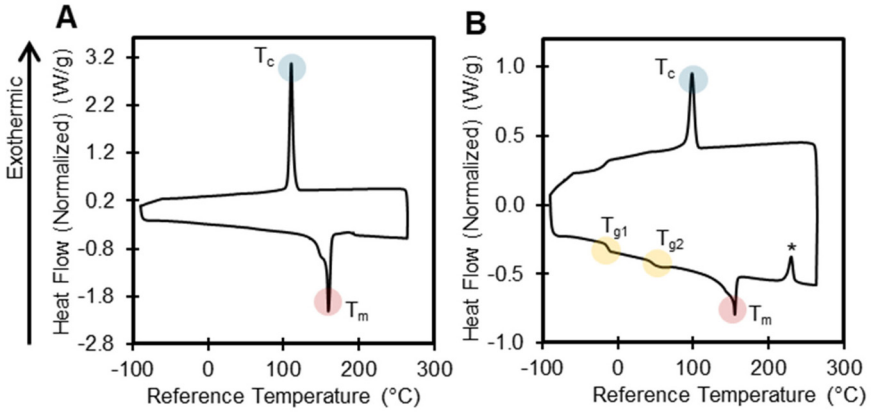

Fig. 8 First heat DSC trace for (A) PP-1, with the melting temperature (T_m) labeled in red and crystallinity temperature (T_c) labeled in blue and (B) PP-2, where two glass transitions were observed (T_{g1}, T_{g2}) labeled in yellow, and an exotherm (*) following the melting endotherm (T_m). The DSC trace of PP-2 indicates a complex polymer morphology and possibly the presence of additives. PP samples were run from −90 °C to 265 °C at a rate of 10 °C min^{-1} with 5-minute isothermal holds between each heating and cooling ramp.

after the melting point at approximately 260 °C and 280 °C, respectively (Fig. S18 and S19†), likely due to the loss of adsorbed water.[84] The DSC thermogram for PP-2, PP-5, PP-6, and PP-7 contained an exotherm after the melting endotherm in the first heat (Fig. 8 and S20–S22†). While there is no corresponding mass loss event in the TGA results, it is likely that crystallization or curing are occurring, possibly due to the presence of additives. We did observe complex low molecular mass wax mixtures in these three PP samples by ASE GC-MS, but it is uncertain what mechanism is causing an exotherm. The DSC chromatogram for PS-5 contained sharp, inconsistent crystallization peaks in both cooling cycles, indicating the presence of impurities (Fig. S23†), with no corresponding mass loss event in TGA data. GC-MS data of PS-5 provides evidence of a complex mixture of aromatics and unknowns that might induce crystallization events.

Certain types of exotherms can indicate structural changes including cyclization and further chemical reactions. For example, the DSC of PAN exhibited an exotherm at 285 °C (Fig. S24†), which is consistent with previous literature results, indicating cyclization reactions that form carbon fibers.[70,85] EVA-1 (25% VA) and EVA-2 (40% VA) both exhibited exotherms that correspond to crosslinking events at 241 °C and 231 °C respectively (Fig. S25 and S26†). Increasing vinyl acetate content lowers the thermal stability of EVA, resulting in lower crosslinking temperatures.[84]

Changes between the first and second heat can provide insight into the applied thermal history, crystallization behavior, and stability of a polymer. Typically, the first heating cycle is used to 'erase' the thermal history of the polymer, allowing the comparison of polymer samples when a controlled thermal history is applied. Examining the first heat of the polymer is most relevant to recycling treatments conducted on polymers as is, while the second heat scan after thermal stress can assess the reversibility of crystallization behavior. For example, several PE, PP, PBT, and PHB samples had slight increases in crystallinity in the second heat (2.3–23.6%) while most EVOH, PVAc, and PVOH plastics exhibited decreases in crystallinity in the second heat (12.0–65.4%), suggesting that the latter polymers have undergone a process of stress relaxation (Fig. 9). These results indicate that performing reactions at or near melt can have significant impacts on the polymer, independent from other viariables. This type of DSC analysis can also be used to understand how thermal pretreatment can impact deconstruction effeciency, such as using melt processing as a pretreatment prior to the enzymatic depolymerization of PET.[86]

Finally, although DSC is useful in determining some of the most pertinent polymer thermal properties, interpretation can be limited when the structure is not known. For example, the PU material also exhibited an exotherm in the first heat at approximately 229 °C (Fig. S27†), which could be due to several unknown processes that might include thermal history, crosslinking, or possibly additives. The TGA scan of the PU material also contained a mass loss event at 263 °C that accounts for approximately 45 wt%, which was confirmed by EGA as likely 1,2-dibutoxyethane, while the GC-MS data indicates the presence of several possible organic additives. These observations highlight the need for multiple techniques to characterize polymer formulations.

Changes in polymer characteristics with cryomilling

After characterizing the polymers as received, we sought to understand the effect of pre-processing techniques. Cryomilling is a common pre-processing technique prior to plastics depolymerization processes because it reduces particle size, and increases porosity and surface area, which can simultaneously impact the thermal properties and molecular mass distributions of the polymer.[16,87] There are two potential effects that cryomilling may have on plastic: stress-induced cracking and stress-induced crystallization.[88] We cryomilled all samples, excluding PU, PK, and polymers that were purchased

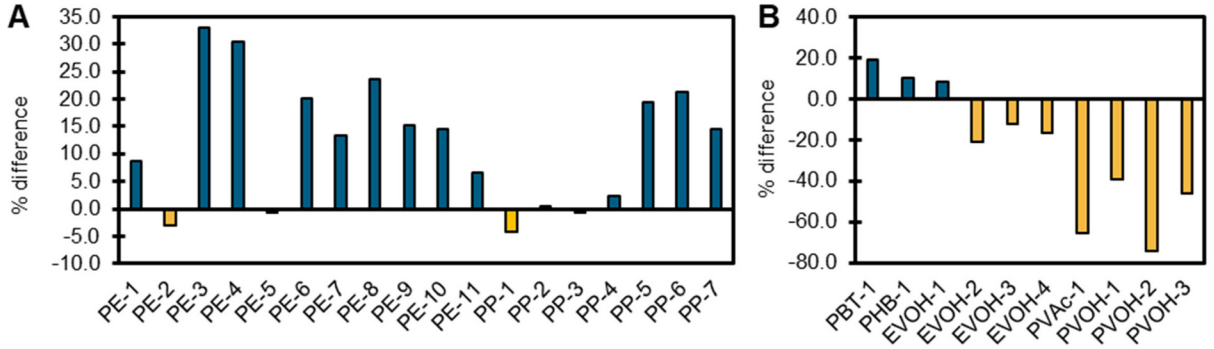

Fig. 9 Changes in percent crystallinity between the first and second heat of a DSC experiment for (A) all PE and PP samples (B) all PBT, PHB, EVOH, PVAc, and PVOH samples. Increasing values indicate an increased cystallinity in the second heat, and decreasing values indicate decreasing crystallinity in the second heat. These results can be used to assess how much thermal history was applied to the polymer, and reversability of crystallization behavior. Samples were run from at a rate of 10 °C min^{-1} with 5-minute isothermal holds between each heating and cooling ramp. Upper and lower temperature bounds can be found in Table S12 in the ESI.†

as powders (see Text S1† for details). In the following section we will discuss polymer changes observed after cryomilling using GPC, DSC, as well as SAXS, and WAXS.

GPC was used to determine changes in molecular mass distributions and dispersity following cryomilling, by correlating changes in molecular mass distributions to the length of time a sample was cryomilled.[89] Changes in M_w, M_n, and $Đ$ post cryomilling was observed in 15 polymers (Fig. 10). Decreases in M_w, M_n, and $Đ$ occurred in three polymers (PE-6, PP-5, and PS-3) indicating that these polymers exhibited a decrease in number and weight-average molecular mass which resulted in a narrower distribution of molecular masses. Alternatively, ABS-1, PMMA-1, PMMA-5, and PVAc-1 exhibited an increase in $Đ$ indicating that the decrease in M_n resulted in a broader distribution of masses. PS-1 had decreases in M_w and M_n with minimal change in $Đ$, indicating that the reduction in average molecular mass did not impact the overall distribution of masses. PVC-2 and PHB-1 displayed an increase in M_n, with a decrease in both M_w and $Đ$, which likely indicates that the higher molecular mass portion of the polymer were reduced to

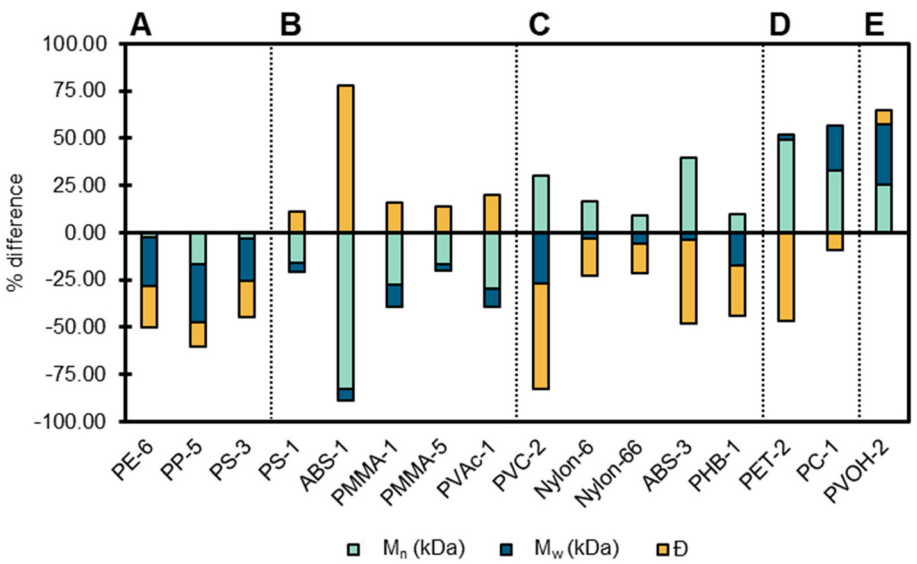

Fig. 10 Percent difference of number-average molecular mass (M_n), weight-average molecular mass (M_w), and dispersity ($Đ$) after cryomilling. Increasing % difference indicates an increase following cryomilling, and polymers shown exhibit differences of >15% in at least one category. (A) M_n, M_w, and $Đ$ all decrease for PE-6, PP-5, and PS-3. (B) M_n and M_w decrease, and $Đ$ increases for PS-1, ABS-1, PMMA-1, PMMA-5, and PVAc-1. (C) M_w and $Đ$ decrease, and M_n increases for PVC-2, nylon-6, nylon-66, ABS-3, and PHB-1. (D) $Đ$ decrease, M_n and M_w increases for PET-2, and PC-1. (E) M_n, M_w, and $Đ$ all increase for PVOH-2. M_n represents the most abundant, often lower, molecular masses, whereas M_w represents the higher molar mass portion of the bulk polymer. A decrease in M_n, M_w, and $Đ$ indicates both a decrease in low and high molecular mass components and distribution of masses.

masses that were higher than previously lower masses contributing to M_n, while narrowing the range of masses present. Several polymers had increases in M_n and decreases in $Đ$ with minimal impact or an increase in M_w (PET-2, ABS-3, Nylon-6, PC-1) indicating that higher molecular mass chains were either preserved or formed, resulting in a narrower distribution of masses. Processes that might contribute to higher molecular masses include re-aggregation, cross-linking, and diffusion of additives to the polymer matrix. It should be noted that ABS and PVC-2 data has higher associated error due to poor solubility and mass recovery of the polymer.

DSC was used to detect changes in crystallization temperatures and percent crystallinity, implying changes in molecular mass or molecular mass distribution. Polymers that displayed increases in percent crystallinity following cryomilling included PET-3, EVOH-1, and nylon-6 (statistically significant at 95% confidence intervals). PET-3 changed from 2.0% to 5.5% crystallinity accompanied by an increase in T_c by 4 °C. PET-3 is amorphous, and in previous studies, cryomilling amorphous PET has resulted in increased crystallinity.[87,89] Increased crystallinity in polymers may occur because mechanical work during cryomilling provides enough heat to overcome the cold crystallization temperatures locally, or from strain mediated crystallization.[88,90] Researchers in one study found that changes induced by cryomilling are primarily physical in nature and can be erased by thermal treatment.[91]

SAXS and WAXS were used to observe structural changes after cryomilling. The SAXS and WAXS patterns obtained for the as-received and cryomilled samples exhibited noticeable distinctions, indicating changes in the multiscale structures of certain polymers. The two primary impacts of cryomilling were changes in the degree of crystallinity, and the development of crystal polymorphs. While we did not observe a change in percent crystallinity for PP-3, PP-5, PP-6, and PLA using DSC, SAXS and WAXS data provide evidence of a decrease in crystallinity for these polymers. Fig. 11 illustrates the SAXS and WAXS patterns for PP-3, comparing the as-received sample with the cryomilled sample. The SAXS data for the cryomilled sample exhibited a less pronounced correlation peak and increase in scattering intensity at the low q-range, in contrast to the as-received sample (Fig. 11A). The increase in low q-range scattering is attributed to the presence of micrometer-size particles due to cryomilling. We attribute the reduction in correlation peak intensity to the loss of crystalline domains due to cracking during cryomilling, which decreases the total volume of scattering centers. The WAXS data (Fig. 11B) further support the observed loss of crystalline domains in the cryomilled sample, evidenced by a decrease in the intensity of characteristic diffraction peaks associated with crystalline domains and increased amorphous domains scattering, consistent with an increased amorphous fraction as compared to the as-received sample.

In addition to reduced crystallinity through cryomilling, samples PE-1, PE-2, PE-7, PE-10, and PE-11 exhibited the appearance of new crystal structures. This is supported by the appearance of distinct new peaks in the WAXS data (Fig. S28–S32†). This is consistent with prior observations that PE can exhibit different crystalline phases as a function of the manufacturing processes, primarily driven by the thermal and pressure history.[92–94] The orthorhombic phase (space group: *Pnam*, unit cell parameters: a = 0.740 nm, b = 0.493 nm, and c = 0.253 nm along the chain axis) is considered the most stable phase.[93] The less stable monoclinic and triclinic phases have been observed in samples subjected to mechanical stress.[92–95] The presence of the new crystalline phase in the cryomilled PE samples suggests that the mechanical stress induced during the cryomilling process was sufficient to induce a phase transformation between the orthorhombic, mono- and tri-clinic phases.

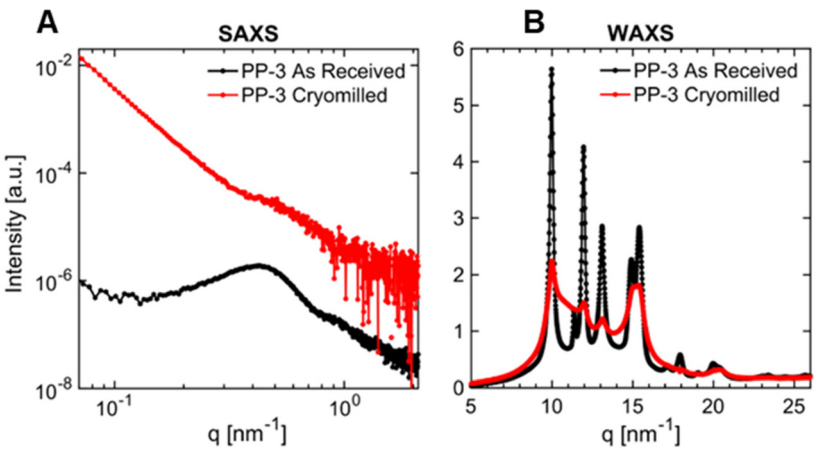

Fig. 11 (A) SAXS X-ray curves and (B) WAXS X-ray curves for comparing cryomilled and as received PP-3. Results indicate a decrease in crystallinity following cryomilling. SAXS measurements were conducted at an X-ray energy of 15 keV (λ = 0.08265 nm) with a sample-to-detector distance (SDD) of 2.8 m, while WAXS measurements were performed at 12.7 keV (λ = 0.09762 nm) with an SDD of 350 mm.

Discussion

It is essential to fully characterize polymers prior to recycling studies to understand and compare results across studies. Polymer properties including crystallinity, molecular mass distribution, and morphology can have potential impacts on deconstruction chemistries. Furthermore, organic and inorganic additives can also impact certain deconstruction chemistries. This study provides a framework of analytical procedures for characterizing polymer properties and the presence of additives, as well as providing a source of fully characterized polymer substrates that can be accessed by the global research community.

Potential impacts of polymer properties on recycling

Molecular mass and dispersity of a polymer can potentially impact the product yields and speciation of products depending on the recycling technology.[79,80,96,97] For example, Celik *et al.* have shown that hydrogenolysis of higher molecular weight PE using a $Pt/SrTiO_3$ catalyst results in higher product yields likely because higher molecular weight PE is preferentially absorbed to the surface of the catalyst.[79] In contrast, Zhang *et al.* converted PE to long-chain di-alkyl aromatics and found that low-density PE had significantly higher yields (70–80%) than high-density PE (55%).[98] Meanwhile, Tennakoon *et al.* developed a $mSiO_2/Pt/MCM$-48 catalyst for hydrogenolysis of PE, which results in similar yields of waxy hydrocarbons from PE of varying molecular mass distributions.[99] Additionally, crystallinity can have a substantial impact on the efficiency of enzymatic depolymerization of PET. Erickson *et al.* found that there is likely an influence of surface area and crystallinity on enzymatic deconstruction reaction rate, but this does not increase the overall conversion extent.[16,100] In solvent-based separation of mixed waste plastics, the dissolution process is impacted by the polymer type, solvent type, as well as the molecular mass,[101] and crystallinity.[97,102–104] In conjunction with these examples, our study highlights the large variation in polymer physical properties among commercial substrates and shows that characterizing prior to recycling studies is essential in understanding these processes.

Potential impacts of additives on recycling

The presence of many additives limits the mechanical recyclability of many plastics,[9,105,106] and may impact polymer deconstruction technologies.[14,107] Additives can also pose a threat to the environment, and regulations may heavily impact the recycling industry.[19,108]

Additives, such as antioxidants, can impact the efficiency of catalytic deconstruction.[14,109] For example, Hinton *et al.* found that the presence of phenolic antioxidants reduced the product yields during catalytic hydrocracking of PE.[14] Several of the polymers analyzed in our study contained similar types of antioxidants, such as organophosphorus antioxidants, many of which would not have been known without characterization. Solvent-based extraction technologies present promising solutions to removing additives prior to recycling.[110] In the same study, Hinton *et al.* found improved yields after solvent stripping a PE containing an antioxidant.[14] Sulfur, halides, cyanides, and nitro compounds are also important to consider because they can be potent metal catalyst poisons.[12,111] The accumulation of toxic additives might also impact the efficiency of bioconversion processes, due to the antibiotic nature of certain additives such as halogenated phenols and antimicrobials.[107]

Additives such as halogenated organics and heavy metals may pose a threat to the environment and can possibly be released during recycling processes.[19,108] For example, low molecular mass fluorinated compounds are likely to impact waste streams as they are difficult to break down and are long lasting in the environment.[112–114] As evidenced by this study, the use of low molecular mass fluoropolymers is likely widespread in other polymer classes. This is becoming increasingly important with evolving total organic fluorine regulations, which do not distinguish between chemical species of fluorinated compounds.[115] Phthalates are another widely used class of additives, and several are regulated in Japan, the European Union, the United States, and Australia, due to their toxicity.[116] While these regulations are compound-specific, it is likely that legacy and newly developed phthalates may continue to pose challenges for recycling technologies. Toxic heavy metals commonly used in the production of plastic may also pose a problem for recycling technologies, including Sb, As, Cd, Co, Cr(VI), Hg, Pb, and Sn.[108] This study also found trace levels of several of these elements in the polymers analyzed (Fig. S3†). For example, Sb_2O_3 is a commonly used catalyst used in the production of PET and is found frequently in PET finished products, but is considered a carcinogen.[61,117] These examples highlight the importance of characterizing plastics for inorganic and organic additives to understand the fate and impact of regulated and toxic additives in recycling technologies.

Limitations and conclusions

We emphasize that these measurements were conducted on a particular set of polymers from specific companies, with provided lot numbers, and it is acknowledged that distributors may change between lot numbers, resulting in different formulations. As plastic physically ages, it can also undergo environmental stress that may change its properties.[118] We also acknowledge that many of the plastics we analyzed contain unknown additives due to the limitations of library matching, and that structural analysis of these additives will require advanced techniques such as high resolution mass spectrometry and NMR. As technologies develop, the use of more complex plastic feedstocks including post-consumer waste of unknown formulations will increase, and while out-of-scope for this study, there has been some work studying the characteristics of mixed plastics from material recovery facilities.[119] Analytical challenges associated with mixed plastic waste includes differentiating complex polymer formulations with

multiple polymer and co-polymer blends, as well as assessing complex additive mixtures.

Overall, this study highlights a suite of analytical approaches to thoroughly characterize polymers for recycling studies, providing the research community with readily accessible fully characterized substrates. Described in detail are important examples of how physical and chemical properties, such as molecular mass and the presence of antioxidants, can impact polymer deconstruction. It is critical for reproducibility and comparisons among studies that the research community consistently and properly characterize plastic substrates to understand the impacts of a polymer's physical properties and chemical composition in recycling studies.

Experimental

Materials and sample preparation

Plastic substrates were purchased from various vendors (Table 1). Reagents and standards were purchased at the highest available purity and can be found in Table S10.† Samples were cryomilled using a Horiba Freezer Mill 6770 (SPEX SamplePrep, Metuchen, NJ, USA) using a SPEX 6751C4 polycarbonate cylinder grinding vial. A detailed procedure can be found in Text S1 in ESI.† Plastic substrates that were not viable for cryomilling include polyurethane (PU) and polyketone (PK).

Fourier-transform infrared spectroscopy (FTIR)

Bulk plastic characterization was conducted using FTIR. Plastic samples were run on a FTIR Spectrum 3 spectrometer (PerkinElmer, Waltham, MA, USA) equipped with a Universal ATR Sampling Accessory. The Universal ATR Sampling Accessory contains a Diamond/ZnSe crystal with one laser bounce. The crystal was cleaned before and after each run with a Kimwipe sprayed with isopropanol (Fisher Scientific, ACS grade). A background spectrum was run before each plastic sample. 10–15 mg of polymer sample was used. Each spectrum was run at ambient temperature with a wavenumber range of 650–4000 cm^{-1}, a resolution of 4 cm^{-1}, and an accumulation of 16 scans. The force gauge was set at 75–80% of maximum pressure. All spectra were analyzed using PerkinElmer Spectrum IR software. Library matching was conducted using KnowItAll Informatics System 2021, Spectroscopy Edition (John Wiley & Sons, Inc.).

Gel permeation chromatography (GPC)

GPC coupled with a MALS and dRI detector were used to determine weight-average molecular mass (M_w), number-average molecular mass (M_n), and dispersity ($Đ$) values for both non-cryomilled and cryomilled plastic substrates. A 1260 Infinity II LC system (Agilent, Santa Clara, CA, USA), consisting of a 1260 Iso pump module, 1260 vial sampler module, and a 1260 Multicolumn Thermosat (MCT) module was used for all room-temperature GPC. M_w, M_n, and $Đ$ for PE, PP, and EVA were measured using high-temperature GPC (HT-GPC) coupled with a dRI detector, on an EcoSec HLC-8321 (Tosoh, Tokyo, Japan). Detailed methods including variations for different plastic substrates can be found in Text S2, S3 and Table S11.†

Differential scanning calorimetry (DSC)

DSC was used to characterize both as-received and cryomilled polymer substrates. DSC measurements were simultaneously performed in triplicate on a Discovery X3 DSC (TA Instruments, New Castle, DE, USA) using 7–10 mg of sample in hermetically sealed aluminum pans (DSC Consumables, Austin, MN, USA). The glass transition temperature (T_g), melting temperature (T_m), enthalpy of melting (ΔH_m), crystallization temperature (T_c), temperature of cold crystallization (T_{cc}), and enthalpy of cold crystallization (ΔH_{cc}) were determined for each polymer substrate when applicable with TRIOS software. Statistical differences were analyzed using the Student's t-test at the 95% confidence interval using a pooled standard deviation (eqn (S2)†). Detailed information about the DSC procedures for each polymer can be found in Text S4, eqn (S1), (S2), and Table S12.†

Thermogravimetric analysis (TGA) and evolved gas analysis (EGA) with TGA-FTIR

Thermogravimetric analysis (TGA) was used to analyze the thermal stability of both as-received and cryomilled polymer substrates. TGA was performed using a Discovery TGA 5500 (TA Instruments) for all polymers except PS-2 which was run on a Discovery SDT 650 (TA Instruments). For each run, 7–10 mg of polymer sample was placed in a platinum TGA pan. Samples were heated under nitrogen from ambient temperature to 200 °C at a rate of 4 °Cmin^{-1}, then from 200 °C to 800 °C at a rate of 20 °Cmin^{-1}. TRIOS software (TA Instruments) was used to characterize the onset temperature of polymer degradation and the weight percent of residue at 800 °C. The weight percent loss and temperature of the derivative maximum were determined for each weight loss event. For samples with only one polymer mass loss event, the temperature at which half of the initial sample weight remained ($T_{d.50}$) was also characterized. Samples that exhibited weight loss events below 200 °C that were greater than 1 wt% were further characterized by EGA. Approximately 7–10 mg of each sample were analyzed using a Discovery SDT 650 instrument (TA Instruments) connected to a FTIR Spectrum 3 spectrometer (PerkinElmer) equipped with a TL 8000 Balanced Flow FTIR EGA System (PerkinElmer). Details on EGA using a hyphenated TGA-FTIR system can be found in Text S5 in the ESI.† Additionally, samples with a residue greater than 1 wt% were further analyzed under air (21% oxygen) to quantify char. For each substrate, 7–9 mg of polymer sample was placed in a high temperature, platinum TGA pan and heated from ambient temperature to 900 °C at rate of 20 °Cmin^{-1} on a Discovery TGA 5500 (TA Instruments). Only the cryomilled form was analyzed, except for cases in which the sample was already a powder or not viable for cryomilling, in which case the as-received substrate was analyzed.

Small and wide-angle X-ray scattering (SAXS and WAXS)

The SAXS and WAXS experiments were performed at beamlines 1-5 and 11-3 of the Stanford Synchrotron Radiation Lightsource (SLAC National Laboratory, Menlo Park, USA), respectively. Powder samples were placed between two thin Kapton® films using washers. Pellet samples were attached to Kapton® tape, while film samples were directly placed on the sample holder for transmission SAXS and WAXS measurements. Backgrounds from Kapton® films, tape, and air were measured for each sample to perform background subtraction during data correction. The SAXS and WAXS data were reduced using the Nika package[120] for Igor Pro (Wavemetrics, Inc., Igor 8.04) to extract a 1D radial profile. Additionally, data correction was performed using MATLAB (R2021a) scripts. Detailed SAXS and WAXS experimental setup, data reduction and correction can be found in Text S6.†

CHNS analysis

The polymer samples were analyzed for carbon, hydrogen, nitrogen, and sulfur (CHNS) using a LECO CHN 628 series with Sulfur Add-on Module (S628) (LECO Corporation; St Joseph, MI, USA). CH and N were measured separately from S using previously established methods.[121–123] Details on these procedures can be found in Text S7 and Table S13.†

Inductively coupled plasma mass spectrometry (ICP-MS)

Samples were screened for 68 elements by inductively coupled plasma mass spectrometry (ICP-MS), before quantification. The initial screen established an approximate estimate for quantification. First, samples were microwave acid wet digested (MAWD) using a ultraWAVE Digester (Milestone, Sorisole, Italy) (Text S8 and Table S14†). Initially, approximately 200 mg of sample were digested in 4 mL of high purity nitric acid (HNO_3), diluted to 3% acid in Milli-Q water, and screened using ICP-MS with high purity standard mixtures as reference. For quantification, approximately 250 mg of sample was digested in 4 mL HNO_3, and 2 mL 50% aqueous tetrafluoroboric acid (HBF_4). Digestates were then diluted in Milli-Q water to 3% acid (0.5 mL in 15 mL total). For halogen analysis of Cl, Br and I, 0.5 mL of samples were diluted in a 15 mL total triethanolamine basic solution. Analysis was conducted on a triple quadrupole ICP-MS (Agilent, Santa Clara, CA, USA) using previously established methods.[124] Elements can have high backgrounds due to instrumental interferences and laboratory background noise including Na, Si, K, and Ca, therefore method blanks were run simultaneously in triplicate, averaged, and samples were blank subtracted. Hg was semi-quantified using a proxy and adjusted based on established instrumental responses, and boron was semi-quantified with a 3-point calibration curve using the HNO_3 digestion screening method as described above.

Fluorine analysis

Samples were sent to Intertek (Whitehouse, NJ) for total fluorine analysis. Briefly, samples were weighed and transferred onto a bed of mannitol wrapped in an ashless filter paper. The sample was then combusted in an oxygen combustion flask containing 100 mL of total ionic strength adjustment buffer II (TISAB II). Following combustion, the sample was equilibrated for 20 min. Total fluorine was then determined potentiometrically with an ion-specific electrode. The electrode was calibrated with a NIST traceable organic standard that contains fluorine prior to analysis, and within ± 0.3% absolute. Percent F was calculated based on the sample weight, solution volume and fluoride concentration.

Accelerated solvent extraction with gas chromatography mass spectrometry (ASE GC-MS)

An organic additive screen was conducted on all substrates using previously established methods utilizing GC-MS with minor adjustments.[37,125] For GC-MS analysis, accelerated solvent extraction (ASE) was conducted using a Model ASE 200 (Dionex, Germany). 500 mg to 1 g of cryomilled sample was mixed with diatomite to fill an ASE extraction cell. Samples were then extracted using 50 : 50 hexane and ethyl acetate as extraction solvents. The oven temperature was 100 °C, with a static time of 15 minutes and run for 2 cycles. The extracted solvent was dried completely under nitrogen, reconstituted with 1 mL of dichloromethane (DCM), and analyzed using a gas chromatography mass spectrometer with a flame ionization detector splitter (GC-MS/FID) on an Agilent 8890 GC coupled to a 5977 EI MSD (Agilent, Santa Clara, CA, USA). Complete methods and conditions for the GC-MS/FID can be found in Text S9 in ESI.†

Pyrolysis gas chromatography mass spectrometry (PyGC-MS)

PyGC-MS was conducted using a tandem micro-furnace PY-2020iS/Rx-5030TR pyrolyzer (Frontier Laboratories, Koriyama, Japan) coupled to a GC-MS/FID (Agilent 7890B/5977A MSD). Approximately 1 mg samples of plastic substrate were loaded into deactivated stainless-steel cups, then automatically dropped into the pyrolysis zone set to 350 °C. The products from the pyrolysis zone were entrained in 54 mL min^{-1} of He carrier gas, then injected into the GC-MS/FID inlet with a liquid nitrogen trap. The condensable vapors were desorbed from the liquid nitrogen trap and separated on an Ultra-Alloy-5 capillary column (Frontier Laboratories, Japan). The GC oven was programmed as follows: hold at 40 °C for 2 min, then ramp to 300 °C at a rate of 10 °C min^{-1} hold for 5 min.

Data processing was conducted on MassHunter Qualitative Analysis 10.0 and MassHunter Unknowns Analysis software (Agilent). Library matching was conducted using NIST 2020 and F-Search libraries. Compounds with a 75% library match were reported, while lower matching percentages were reported as unknown. Library matching is considered tentatively identified, and compounds were not confirmed with standards.

Data availability

The ESI† includes all graphs, figures, and methods referenced in this manuscript. All data collected for each polymer can be

accessed on an open access database named "BOTTLE Plastic Substrates Database" on plus.figshare.com.

Author contributions

Conceptualization: AAC, CJT, NAR, GTB. Methodology: AAC, CL, JM, LMS, AKM, CJT, NAR, GTB. Investigation: AAC, CL, JM, LMS, AKM, ASA. Data Curation: AAC, CL, JM, LMS, AKM. Writing – original draft: AAC. Writing – reviewing and editing: AAC, CL, JM, LMS, AKM, CJT, NAR, GTB. Visualization: AAC. Supervision: CJT, NAR, GTB. Funding acquisition: CJT, NAR, GTB.

Conflicts of interest

The authors declare no conflicts of interest.

Acknowledgements

We thank David Moore for running ICP-MS analysis on all samples. We thank Elizabeth Stone and Kathy Cisar for the TOC image. We thank Bill Michener, Kelly Orton, and Ryan Ness for instrumental support on ASE, GC-MS/FID, and PyGC-MS and for helpful discussions. We thank Karl Weitz and the team at the Environment Molecular Laboratory Sciences (EMSL) at PNNL for running high resolution GC-MS. We also thank Dr Amani M. Ebrahim of the SLAC for beamtime support. We thank Dr Anna Walsh for the suggestions on Fig. 3.

This material was partially based upon work supported by the U.S. Department of Energy, Office of Energy Efficiency and Renewable Energy, Bioenergy Technologies Office (BETO) under Award Number DE-EE-0009285.

Funding was partially provided by the U.S. Department of Energy, Office of Energy Efficiency and Renewable Energy, Advanced Materials and Manufacturing Technologies Office (AMMTO) and Bioenergy Technologies Office (BETO). This work was performed as part of the Bio-Optimized Technologies to keep Thermoplastics out of Landfills and the Environment (BOTTLE) Consortium and was supported by AMMTO and BETO under Contract DE-AC36-08GO28308 with the National Renewable Energy Laboratory (NREL), operated by Alliance for Sustainable Energy, LLC. Use of the Stanford Synchrotron Radiation Lightsource, SLAC National Accelerator Laboratory, is supported by the U.S. Department of Energy, Office of Science, Office of Basic Energy Sciences under contract no. DE-AC02-76SF00515.

The views expressed in the article do not necessarily represent the views of the DOE or the U.S. Government. The U.S. Government retains and the publisher, by accepting the article for publication, acknowledges that the U.S. Government retains a nonexclusive, paid-up, irrevocable, worldwide license to publish or reproduce the published form of this work, or allow others to do so, for U.S. Government purposes.

References

1 L. D. Ellis, N. A. Rorrer, K. P. Sullivan, M. Otto, J. E. McGeehan, Y. Román-Leshkov, N. Wierckx and G. T. Beckham, *Nat. Catal.*, 2021, **4**, 539–556.
2 C. I. Idumah, *J. Therm. Anal. Calorim.*, 2022, **147**, 3495–3508.
3 Y. Peng, Y. Wang, L. Ke, L. Dai, Q. Wu, K. Cobb, Y. Zeng, R. Zou, Y. Liu and R. Ruan, *Energy Convers. Manage.*, 2022, **254**, 115243.
4 A. Mohanty, R. K. Borah, A. P. Fatrekar, S. Krishnan and A. A. Vernekar, *Chem. Commun.*, 2021, **57**, 10277–10291.
5 S. C. Kosloski-Oh, Z. A. Wood, Y. Manjarrez, J. P. de los Rios and M. E. Fieser, *Mater. Horiz.*, 2021, **8**, 1084–1129.
6 K. Ragaert, L. Delva and K. Van Geem, *Waste Manage.*, 2017, **69**, 24–58.
7 H. Li, H. A. Aguirre-Villegas, R. D. Allen, X. Bai, C. H. Benson, G. T. Beckham, S. L. Bradshaw, J. L. Brown, R. C. Brown, V. S. Cecon, J. B. Curley, G. W. Curtzwiler, S. Dong, S. Gaddameedi, J. E. García, I. Hermans, M. S. Kim, J. Ma, L. O. Mark, M. Mavrikakis, O. O. Olafasakin, T. A. Osswald, K. G. Papanikolaou, H. Radhakrishnan, M. A. Sanchez Castillo, K. L. Sánchez-Rivera, K. N. Tumu, R. C. Van Lehn, K. L. Vorst, M. M. Wright, J. Wu, V. M. Zavala, P. Zhou and G. W. Huber, *Green Chem.*, 2022, **24**, 8899–9002.
8 J. M. Garcia and M. L. Robertson, *Science*, 2017, **358**, 870–872.
9 Z. O. G. Schyns and M. P. Shaver, *Macromol. Rapid Commun.*, 2021, **42**, 2000415.
10 P. Benyathiar, P. Kumar, G. Carpenter, J. Brace and D. K. Mishra, *Polymers*, 2022, **14**, 2366.
11 R. Geyer, J. R. Jambeck and K. L. Law, *Sci. Adv.*, 2017, **3**, e1700782.
12 M. D. Argyle and C. H. Bartholomew, *Catalysts*, 2015, **5**, 145–269.
13 A. C. Jerdy, T. Pham, M. Á. González-Borja, P. Atallah, D. Soules, R. Abbott, L. Lobban and S. Crossley, *Appl. Catal., B*, 2023, **325**, 122348.
14 Z. R. Hinton, P. A. Kots, M. Soukaseum, B. C. Vance, D. G. Vlachos, T. H. Epps and L. T. J. Korley, *Green Chem.*, 2022, **24**, 7332–7339.
15 R. A. Hackler, J. V. Lamb, I. L. Peczak, R. M. Kennedy, U. Kanbur, A. M. LaPointe, K. R. Poeppelmeier, A. D. Sadow and M. Delferro, *Macromolecules*, 2022, **55**, 6801–6810.
16 R. K. Brizendine, E. Erickson, S. J. Haugen, K. J. Ramirez, J. Miscall, D. Salvachúa, A. R. Pickford, M. J. Sobkowicz, J. E. McGeehan and G. T. Beckham, *ACS Sustainable Chem. Eng.*, 2022, **10**, 9131–9140.
17 S. R. Nicholson, N. A. Rorrer, A. C. Carpenter and G. T. Beckham, *Joule*, 2021, **5**, 673–686.
18 H. Wiesinger, Z. Wang and S. Hellweg, *Environ. Sci. Technol.*, 2021, **55**, 9339–9351.
19 J. N. Hahladakis, C. A. Velis, R. Weber, E. Iacovidou and P. Purnell, *J. Hazard. Mater.*, 2018, **344**, 179–199.

20 A. N. Walsh, C. M. Reddy, S. F. Niles, A. M. McKenna, C. M. Hansel and C. P. Ward, *Environ. Sci. Technol.*, 2021, **55**, 12383–12392.
21 L. Hermabessiere, A. Dehaut, I. Paul-Pont, C. Lacroix, R. Jezequel, P. Soudant and G. Duflos, *Chemosphere*, 2017, **182**, 781–793.
22 W. C. Li, H. F. Tse and L. Fok, *Sci. Total Environ.*, 2016, **566–567**, 333–349.
23 H. Luo, C. Liu, D. He, J. Sun, J. Li and X. Pan, *Sci. Total Environ.*, 2022, **849**, 157951.
24 Nurlatifah, T. Yamauchi, R. Nakajima, M. Tsuchiya, A. Yabuki, T. Kitahashi, Y. Nagano, N. Isobe and H. Nakata, *Sci. Total Environ.*, 2021, **768**, 144537.
25 V. García Ibarra, A. Rodríguez Bernaldo de Quirós, P. Paseiro Losada and R. Sendón, *Food Packag. Shelf Life*, 2019, **21**, 100325.
26 T. Diera, A. H. Thomsen, S. Tisler, L. T. Karlby, P. Christensen, P. S. Rosshaug, H.-J. Albrechtsen and J. H. Christensen, *Water Res.*, 2023, **229**, 119480.
27 V. P. Sica, K. L. Krivos, D. E. Kiehl, C. J. Pulliam, I. D. Henry and T. R. Baker, *Mass Spectrom. Rev.*, 2020, **39**, 212–226.
28 D. K. Schneiderman and M. A. Hillmyer, *Macromolecules*, 2017, **50**, 3733–3749.
29 G. W. Coates and Y. D. Y. L. Getzler, *Nat. Rev. Mater.*, 2020, **5**, 501–516.
30 M. Hong and E. Y. X. Chen, *Green Chem.*, 2017, **19**, 3692–3706.
31 T. H. Epps III, L. T. J. Korley, T. Yan, K. L. Beers and T. M. Burt, *JACS Au*, 2022, **2**, 3–11.
32 J. Payne and M. D. Jones, *ChemSusChem*, 2021, **14**, 4041–4070.
33 M. M. Abu-Omar, K. Barta, G. T. Beckham, J. S. Luterbacher, J. Ralph, R. Rinaldi, Y. Román-Leshkov, J. S. M. Samec, B. F. Sels and F. Wang, *Energy Environ. Sci.*, 2021, **14**, 262–292.
34 S. J. Pickering, *Composites, Part A*, 2006, **37**, 1206–1215.
35 P. Jagadeesh, S. Mavinkere Rangappa, S. Siengchin, M. Puttegowda, S. M. K. Thiagamani, G. Rajeshkumar, M. Hemath Kumar, O. P. Oladijo, V. Fiore and M. M. Moure Cuadrado, *Polym. Compos.*, 2022, **43**, 5831–5862.
36 C. Moreta and M.-T. Tena, *J. Chromatogr., A*, 2015, **1414**, 77–87.
37 F. Akoueson, C. Chbib, S. Monchy, I. Paul-Pont, P. Doyen, A. Dehaut and G. Duflos, *Sci. Total Environ.*, 2021, **773**, 145073.
38 K. Nahan, E. M. Sussman, B. Oktem, L. Schultheis and S. Wickramasekara, *Talanta*, 2020, **212**, 120464.
39 J. A. Hiltz, *J. Anal. Appl. Pyrolysis*, 2000, **55**, 135–150.
40 X.-S. Luo, J.-B. Huang, L. Wu, L. Jin, W.-W. Xu and X. Yan, *J. Fuel Chem. Technol.*, 2023, **51**, 388–403.
41 A. Parodi, M. D'Ambrosio, L. Mazzocchetti, G. A. Martinez, C. Samorì, C. Torri and P. Galletti, *ACS Sustainable Chem. Eng.*, 2021, **9**, 12575–12583.
42 A. Parodi, A. Jorea, M. Fagnoni, D. Ravelli, C. Samorì, C. Torri and P. Galletti, *Green Chem.*, 2021, **23**, 3420–3427.
43 C. Samorì, G. A. Martinez, L. Bertin, G. Pagliano, A. Parodi, C. Torri and P. Galletti, *Resour., Conserv. Recycl.*, 2022, **178**, 106082.
44 J. K. Lee, K.-B. Kim, J. D. Lee, C. Y. Shin, S. J. Kwack, B.-M. Lee and J. Y. Lee, *Toxicol. Res.*, 2019, **35**, 119–129.
45 C. A. J. Hoeve, H. L. Wagner and P. H. Verdier, *J. Res. Natl. Bur. Stand., Sect. A*, 1972, **76**, 137–140.
46 L. D. Ellis, S. V. Orski, G. A. Kenlaw, A. G. Norman, K. L. Beers, Y. Román-Leshkov and G. T. Beckham, *ACS Sustainable Chem. Eng.*, 2021, **9**, 623–628.
47 S. Huppertsberg and T. P. Knepper, *Anal. Bioanal. Chem.*, 2018, **410**, 6343–6352.
48 G. Celichowski, L. Margielewski and S. Plaza, *Analyst*, 1995, **120**, 2273–2275.
49 L. Kanerva, T. Estlander and R. Jolanki, *Contact Dermatitis*, 1994, **31**, 242–248.
50 Y. Labat, *Phosphorus, Sulfur Silicon Relat. Elem.*, 1993, **74**, 173–194.
51 K. K. Childress, M. D. Alim, J. J. Hernandez, J. W. Stansbury and C. N. Bowman, *Polym. Chem.*, 2020, **11**, 39–46.
52 Y. Shao-Peng, W. Tie-Ning, S. Jiang-Bo, Z. Ye, L. Xiao-Wei and F. Guang-Sheng, *Chin. Phys. Lett.*, 2013, **30**, 108401.
53 C. Postigo and D. Barceló, *Sci. Total Environ.*, 2015, **503–504**, 32–47.
54 L. Lei and I. Aoyama, *Ecotoxicology*, 2010, **19**, 1268–1276.
55 A. B. Morgan and J. W. Gilman, *Fire Mater.*, 2013, **37**, 259–279.
56 A. B. Morgan, *Polym. Rev.*, 2019, **59**, 25–54.
57 K. K. Shen and R. O'Connor, in *Plastics Additives: An A-Z reference*, ed. G. Pritchard, Springer Netherlands, Dordrecht, 1998, pp. 268–276. DOI: **10.1007/978-94-011-5862-6_30**.
58 J. Troitzsch, *Makromol. Chem., Macromol. Symp.*, 1993, **74**, 125–135.
59 J. A. S. Puente, A. Esposito, F. Chivrac and E. Dargent, *J. Appl. Polym. Sci.*, 2013, **128**, 2586–2594.
60 C. F. Struller, P. J. Kelly and N. J. Copeland, *Surf. Coat. Technol.*, 2014, **241**, 130–137.
61 P. Westerhoff, P. Prapaipong, E. Shock and A. Hillaireau, *Water Res.*, 2008, **42**, 551–556.
62 K. K. Shen, S. Kochesfahani and F. Jouffret, *Polym. Adv. Technol.*, 2008, **19**, 469–474.
63 Titanium Dioxide, *S&P Global's Chemical Economics Handbook*, 2021.
64 E. P. Jahrman, G. T. Seidler and J. R. Sieber, *Anal. Chem.*, 2018, **90**, 6587–6593.
65 B. R. Golla, M. Tummala, P. S. Akhil and A. R. James, *Polym. Compos.*, 2019, **40**, 749–757.
66 S. Ebnesajjad, in *Introduction to Fluoropolymers*, William Andrew Publishing, Oxford, 2013, pp. 125–131.
67 Y. Guida, R. Capella and R. Weber, *Emerging Contam.*, 2020, **6**, 143–154.
68 G. J. P. Deblonde, A. B. Kersting and M. Zavarin, *Commun. Chem.*, 2020, **3**, 167.

69 H. M. Ng, N. M. Saidi, F. S. Omar, K. Ramesh, S. Ramesh and S. Bashir, in *Encyclopedia of Polymer Science and Technology*, 2012, pp. 1–29.
70 S. Hajir Bahrami, P. Bajaj and K. Sen, *J. Appl. Polym. Sci.*, 2003, **88**, 685–698.
71 R. A. Mensah, V. Shanmugam, S. Narayanan, J. S. Renner, K. Babu, R. E. Neisiany, M. Försth, G. Sas and O. Das, *Polym. Test.*, 2022, **108**, 107511.
72 K. Kang, Y. Chang, J. C. Choi, S.-J. Park and J. Han, *J. Food Sci.*, 2018, **83**, 1005–1010.
73 C. Janiak and P.-G. Lassahn, *Macromol. Rapid Commun.*, 2001, **22**, 479–493.
74 K. M. K. Ishak, Z. Ahmad and H. M. Akil, *e-Polym.*, 2010, **10**, 64.
75 H. Fleurent and S. Thijs, *J. Cell. Plast.*, 1995, **31**, 580–599.
76 J. M. Chalmers and N. J. Everall, in *Handbook of Vibrational Spectroscopy*, 2001.
77 R. W. Nunes, J. R. Martin and J. F. Johnson, *Polym. Eng. Sci.*, 1982, **22**, 205–228.
78 M. M. Abdelghafour, Á. Orbán, Á. Deák, Ł. Lamch, É. Frank, R. Nagy, A. Ádám, P. Sipos, E. Farkas, F. Bari and L. Janovák, *Polymers*, 2021, **13**, 2725.
79 G. Celik, R. M. Kennedy, R. A. Hackler, M. Ferrandon, A. Tennakoon, S. Patnaik, A. M. LaPointe, S. C. Ammal, A. Heyden, F. A. Perras, M. Pruski, S. L. Scott, K. R. Poeppelmeier, A. D. Sadow and M. Delferro, *ACS Cent. Sci.*, 2019, **5**, 1795–1803.
80 B. M. Stadler and J. G. de Vries, *Philos. Trans. R. Soc., A*, 2021, **379**, 20200341–20200341.
81 I. Fraga, S. Montserrat and J. Hutchinson, *J. Therm. Anal. Calorim.*, 2007, **87**, 119–124.
82 D. R. Burfield and Y. Doi, *Macromolecules*, 1983, **16**, 702–704.
83 A. Vallés-Lluch, W. Camacho, A. Ribes-Greus and S. Karlsson, *J. Appl. Polym. Sci.*, 2002, **85**, 2211–2218.
84 K. Wang and Q. Deng, *Polymers*, 2019, **11**, 1055.
85 H. Liu, S. Zhang, J. Yang, M. Ji, J. Yu, M. Wang, X. Chai, B. Yang, C. Zhu and J. Xu, *Polymers*, 2019, **11**, 1150.
86 A. C. Chang, A. Patel, S. Perry, Y. V. Soong, C. Ayafor, H.-W. Wong, D. Xie and M. J. Sobkowicz, *Macromol. Rapid Commun.*, 2022, **43**, 2100929.
87 F. Kawai, Y. Furushima, N. Mochizuki, N. Muraki, M. Yamashita, A. Iida, R. Mamoto, T. Tosha, R. Iizuka and S. Kitajima, *AMB Express*, 2022, **12**, 134.
88 I. J. Rao and K. R. Rajagopal, *Int. J. Solids Struct.*, 2001, **38**, 1149–1167.
89 Y. G. Zhu, Z. Q. Li, D. Zhang and T. Tanimoto, *J. Appl. Polym. Sci.*, 2006, **99**, 2868–2873.
90 A. P. Cysne Barbosa, M. Stranz, F. Katzenberg and U. Köster, *e-Polym.*, 2009, **9**, 096.
91 C. Bai, R. J. Spontak, C. C. Koch, C. K. Saw and C. M. Balik, *Polymer*, 2000, **41**, 7147–7157.
92 P. W. Teare and D. R. Holmes, *J. Polym. Sci.*, 1957, **24**, 496–499.
93 C. W. Bunn, *Trans. Faraday Soc.*, 1939, **35**, 482–491.
94 D. C. Bassett, S. Block and G. J. Piermarini, *J. Appl. Phys.*, 2003, **45**, 4146–4150.
95 I. A. Strelnikov and E. A. Zubova, *Macromol. Res.*, 2021, **29**, 851–854.
96 S. S. Borkar, R. Helmer, F. Mahnaz, W. Majzoub, W. Mahmoud, M. M. Al-Rawashdeh and M. Shetty, *Chem Catal.*, 2022, **2**, 3320–3356.
97 Y.-B. Zhao, X.-D. Lv and H.-G. Ni, *Chemosphere*, 2018, **209**, 707–720.
98 F. Zhang, M. Zeng, R. D. Yappert, J. Sun, Y.-H. Lee, A. M. LaPointe, B. Peters, M. M. Abu-Omar and S. L. Scott, *Science*, 2020, **370**, 437–441.
99 A. Tennakoon, X. Wu, M. Meirow, D. Howell, J. Willmon, J. Yu, J. V. Lamb, M. Delferro, E. Luijten, W. Huang and A. D. Sadow, *J. Am. Chem. Soc.*, 2023, **145**, 17936–17944.
100 E. Erickson, T. J. Shakespeare, F. Bratti, B. L. Buss, R. Graham, M. A. Hawkins, G. König, W. E. Michener, J. Miscall, K. J. Ramirez, N. A. Rorrer, M. Zahn, A. R. Pickford, J. E. McGeehan and G. T. Beckham, *ChemSusChem*, 2022, **15**, e202101932.
101 C. Gutiérrez, M. T. García, I. Gracia, A. de Lucas and J. F. Rodríguez, *Waste Biomass Valorization*, 2013, **4**, 29–36.
102 K. L. Sánchez-Rivera, A. D. C. Munguía-López, P. Zhou, V. S. Cecon, J. Yu, K. Nelson, D. Miller, S. Grey, Z. Xu, E. Bar-Ziv, K. L. Vorst, G. W. Curtzwiler, R. C. Van Lehn, V. M. Zavala and G. W. Huber, *Resour., Conserv. Recycl.*, 2023, **197**, 107086.
103 V. S. Cecon, G. W. Curtzwiler and K. L. Vorst, *Macromol. Mater. Eng.*, 2022, **307**, 2200346.
104 T. W. Walker, N. Frelka, Z. Shen, A. K. Chew, J. Banick, S. Grey, M. S. Kim, J. A. Dumesic, R. C. Van Lehn and G. W. Huber, *Sci. Adv.*, 2020, **6**, eaba7599.
105 A. Alassali, C. Picuno, Z. K. Chong, J. Guo, R. Maletz and K. Kuchta, *Sustainability*, 2021, **13**, 13266.
106 B. D. Vogt, K. K. Stokes and S. K. Kumar, *ACS Appl. Polym. Mater.*, 2021, **3**, 4325–4346.
107 A. Gluth, Z. Xu, L. S. Fifield and B. Yang, *Renewable Sustainable Energy Rev.*, 2022, **170**, 112966.
108 A. Turner and M. Filella, *Environ. Int.*, 2021, **156**, 106622–106622.
109 J. Wei, J. Liu, W. Zeng, Z. Dong, J. Song, S. Liu and G. Liu, *Catal. Sci. Technol.*, 2023, **13**, 1258–1280.
110 S. Ügdüler, K. M. Van Geem, M. Roosen, E. I. P. Delbeke and S. De Meester, *Waste Manage.*, 2020, **104**, 148–182.
111 P. Forzatti and L. Lietti, *Catal. Today*, 1999, **52**, 165–181.
112 L. A. Schaider, S. A. Balan, A. Blum, D. Q. Andrews, M. J. Strynar, M. E. Dickinson, D. M. Lunderberg, J. R. Lang and G. F. Peaslee, *Environ. Sci. Technol. Lett.*, 2017, **4**, 105–111.
113 J.-W. Kim, N. M. Tue, T. Isobe, K. Misaki, S. Takahashi, P. H. Viet and S. Tanabe, *Environ. Monit. Assess.*, 2013, **185**, 2909–2919.
114 L. Minet, Z. Wang, A. Shalin, T. A. Bruton, A. Blum, G. F. Peaslee, H. Schwartz-Narbonne, M. Venier, H. Whitehead, Y. Wu and M. L. Diamond, *Environ. Sci.: Processes Impacts*, 2022, **24**, 2032–2042.
115 T. Thomas, A. Malek, J. Arokianathar, E. Haddad and J. Matthew, *Intern. Chem. Regul. Law Rev.*, 2023, **6**, 3–17.

116 Y. Wang and H. Qian, *Healthcare*, 2021, **9**, 603.
117 M. Filella, *Chemosphere*, 2020, **261**, 127732.
118 J. A. Harvey, in *Handbook of Environmental Degradation of Materials*, ed. M. Kutz, William Andrew Publishing, Norwich, NY, 2005, pp. 153–163.
119 V. S. Cecon, G. W. Curtzwiler and K. L. Vorst, *Waste Manage.*, 2023, **171**, 313–323.
120 J. Ilavsky, *J. Appl. Crystallogr.*, 2012, **45**, 324–328.
121 LECO Corporation, *Sulfur in Hydrocarbons*, St Joseph, MI, 2014.
122 LECO Corporation, *Determination of Carbon, Hydrogen, and Nitrogen in Biomass*, St Joseph, MI, 2016.
123 J. Miscall, E. D. Christensen, J. Oldstad, S. Deutch and J. R. Ferrell *III, Determination of Carbon, Hydrogen, Nitrogen, and Oxygen in Bio-Oils*, p. 2021.
124 N. Belkouteb, H. Schroeder, J. Arndt, J. G. Wiederhold, T. A. Ternes and L. Duester, *Chemosphere*, 2023, **320**, 138053.
125 N. Dorival-García, F. Galbiati, R. Kruell, R. Kovasy, S. O. Dunne, K. D'Silva and J. Bones, *Talanta*, 2020, **219**, 121198.